AD-779 933

# SEISMIC WAVE PROPAGATION AND EARTHQUAKE CHARACTERISTICS IN ASIA

C. Kisslinger, et al

Cooperative Institute for Research in Environmental Science

Prepared for:

Air Force Office of Scientific Research
Advanced Research Projects Agency

30 April 1974

DISTRIBUTED BY:

NTIS
National Technical Information Service
U. S. DEPARTMENT OF COMMERCE
5285 Port Royal Road, Springfield Va. 22151

i

UNCLASSIFIED

SECURITY CLASSIFICATION OF THIS PAGE (When Data Entered)

AD-779 933

| REPORT DOCUMENTATION PAGE | | READ INSTRUCTIONS BEFORE COMPLETING FORM |
|---|---|---|
| 1. REPORT NUMBER<br>AFOSR - TR - 74 - 0866 | 2. GOVT ACCESSION NO. | 3. RECIPIENT'S CATALOG NUMBER |
| 4. TITLE (and Subtitle)<br>SEISMIC WAVE PROPAGATION AND EARTHQUAKE CHARACTERISTICS IN ASIA. | | 5. TYPE OF REPORT & PERIOD COVERED<br>Semi-annual technical report<br>1 October 1973-31 March '74 |
| | | 6. PERFORMING ORG. REPORT NUMBER |
| 7. AUTHOR(s)<br>C. Kisslinger, E. R. Engdahl, G. Boucher, and R. Ganse | | 8. CONTRACT OR GRANT NUMBER(s)<br>F44620-74-C-0015 |
| 9. PERFORMING ORGANIZATION NAME AND ADDRESS<br>CIRES<br>University of Colorado<br>Boulder, Colorado, 80302 | | 10. PROGRAM ELEMENT, PROJECT, TASK AREA & WORK UNIT NUMBERS<br>ARPA Order 1827<br>Program Code 4F10<br>Program Element 62701E |
| 11. CONTROLLING OFFICE NAME AND ADDRESS<br>Advanced Research Projects Agency/NMR<br>1400 Wilson Boulevard<br>Arlington, VA 22209 | | 12. REPORT DATE<br>30 April 1974 |
| | | 13. NUMBER OF PAGES<br>65 |
| 14. MONITORING AGENCY NAME & ADDRESS(if different from Controlling Office)<br>Air Force Office of Scientific Research/NP<br>1400 Wilson Boulevard<br>Arlington, VA 22209 | | 15. SECURITY CLASS. (of this report)<br>UNCLASSIFIED |
| | | 15a. DECLASSIFICATION/DOWNGRADING SCHEDULE |

16. DISTRIBUTION STATEMENT (of this Report)

Approved for public release; distribution unlimited.

17. DISTRIBUTION STATEMENT (of the abstract entered in Block 20, if different from Report)

18. SUPPLEMENTARY NOTES

19. KEY WORDS (Continue on reverse side if necessary and identify by block number)

Seismic ray tracing
Long-period body waves
Asian earthquakes
Upper mantle structure



20. ABSTRACT (Continue on reverse side if necessary and identify by block number)

Three-dimensional seismic ray tracing leads to improved hypocenter locations and focal mechanism solutions. Relations of events to upper mantle structure to under the Aleutian arc are classified. Long-period P waves are very weak on HGLP seismograms of explosions, but long-period SV waves are seen. Long period body wave spectra can be used to fix the depth of crustal earthquakes. Body wave spectra, magnitudes, and focal mechanisms for events in from seismic zones of central Asia have been determined.

DD FORM 1 JAN 73 1473 EDITION OF 1 NOV 65 IS OBSOLETE

UNCLASSIFIED

SECURITY CLASSIFICATION OF THIS PAGE (When Data Entered)

ARPA Order 1827
Program Code 4F10
Name of Contractor: University of Colorado
Effective Date of Contract: 1 Oct. 1973
Contract Expiration Date: 30 Sept. 1974
Amount of Contract: $100,070
Contract Number: F44620-74-C-0015
Principal Investigator: Carl Kisslinger. (303) 443-2211
Program Manager: William Best
Title of Work: Seismic Waves Propagation and
Earthquake Characteristics in Asia.

Semi-Annual Technical Report No. 1
1 October 1973 - 31 March 1974

C. Kisslinger, E. R. Engdahl, G. Boucher and R. Ganse

30 April 1974



Sponsored by
Advanced Research Projects Agency
ARPA Order No. 1827

## TABLE OF CONTENTS

# Technical Report Summary

The research undertaken in this project is directed to three principal tasks. The first of these is the application of three-dimensional seismic ray tracing to problems of hypocenter location and focal mechanism determination, thereby freeing the analyst from the unrealistic assumptions of a spherically symmetric earth. One of the products of this task will be a greatly improved model of upper mantle structure and wave propagation under the Hindu Kush region of central Asia. The second major task is generally directed to exploring the full capabilities offered by the High Gain Long Period network for discrimination of earthquakes and explosions, especially at low energy levels. The third task is an attempt to establish a classification of Asian earthquakes in interesting source regions on the basis of spectral content, dominant focal mechanism, b- values, and other descriptors.

The principal achievements to date under the first task are the completion of the development of a computer code to treat ray tracing in a generally heterogeneous medium and the successful testing of this code by application to the central part of the Aleutian arc. Significant improvement in hypocenter locations and greatly increased ability to relate the events to the major structural elements have been achieved. The effects of upper mantle structure on focal mechanism solutions and $dT/d\Delta$ measurements at teleseismic distances has also been studied, with results presented in this report.

## Technical Report Summary

The research undertaken in this project is directed to three principal tasks. The first of these is the application of three-dimensional seismic ray tracing to problems of hypocenter location and focal mechanism determination, thereby freeing the analyst from the unrealistic assumptions of a spherically symmetric earth. One of the products of this task will be a greatly improved model of upper mantle structure and wave propagation under the Hindu Kush region of central Asia. The second major task is generally directed to exploring the full capabilities offered by the High Gain Long Period network for discrimination of earthquakes and explosions, especially at low energy levels. The third task is an attempt to establish a classification of Asian earthquakes in interesting source regions on the basis of spectral content, dominant focal mechanism, b- values, and other descriptors.

The principal achievements to date under the first task are the completion of the development of a computer code to treat ray tracing in a generally heterogeneous medium and the successful testing of this code by application to the central part of the Aleutian arc. Significant improvement in hypocenter locations and greatly increased ability to relate the events to the major structural elements have been achieved. The effects of upper mantle structure on focal mechanism solutions and $dT/d\Delta$ measurements at teleseismic distances has also been studied, with results presented in this report.

An associated effort under this task is the investigation of mean P travel-time residuals at stations of the Soviet seismographic network. These results will be used as part of the input for the development of models of crustal and upper mantle structures in central Asia.

Work on long-period body waves has developed along two lines. Spectra of body waves from crustal events recorded on standard long-period instruments of the WWSSN have been interpreted in terms of focal depth. Data from the HGLP network will be used for this purpose also, but that system is not yet up to full operational status. Studies to date of explosion and earthquake seismograms from the HGLP network have revealed that long-period P waves are essentailly absent of explosions, but SV type body waves are strongly generated and are the only body wave type clearly seen on the HGLP records.

Under the third task, P and S wave spectra, magnitudes (long and short-period body wave magnitudes and surface wave magnitudes), and focal mechanisms have been derived for events occuring in from selected source regions of central Asia. This task is still in the data-gathering and basic analysis stage and no general conclusions have been reached.

## 1. Applications of Seismic Ray Tracing

E. R. Engdahl

The problem of ray tracing in a generally heterogeneous medium has been treated using the calculus of variations and Fermat's principle of stationary time. The solution in geocentric spherical polar coordinates is a system of five simultaneous first-order differential equations giving the variation with time of the position $(r, \theta, \phi)$ of a point on a ray and the direction of propagation ($i$ = incident angle, $\alpha$ = azimuth) from this point in terms of the wave speed ($v$) and its spatial derivatives in the medium[1].

A computer program has been developed to treat this generalized formulation. Only the size of computer core and time requirements limit the detail to which v and its spatial derivatives can be represented in the model. To study subduction zones, such as the Kurile-Kamchatka arc, it is convenient to represent the structure with a two-dimensional grid, normal to the arc, in which velocities are specified at discrete points. In this system any degree of structural complexity may be represented, limited only by the fineness of intervals between grid points. The wave speed and its derivatives may then be determined numerically at any point within the structure by using cubic splines.

It has been instructive to study a short slab like the Aleutian arc, which has reasonably well-known geometric parameters, before proceeding to the longer slab of the Kurile-Kamchatka arc. Moreover, the

existence of good data from a local network in the Central Aleutians provides a unique opportunity to study a range of possible models and plate effects that have application elsewhere.

Fig. 1.1 is a cross-section of thirty-nine intermediate depth earthquakes of magnitude 4 or greater which have been located using only data from a local network centered on Amchitka Island in the Central Aleutians and with a Herrin spherically symmetric Earth model. A hypothetical plate model, shown for reference, was independently derived from observed travel times and amplitudes from nuclear explosions on Amchitka Island[2,3]. The scattering of the hypocenters serves to illustrate uncorrected plate effects in the local data. The solid circles are two events within the set which were also relocated but with a common network of twenty-nine local and teleseismic stations. In addition, an attempt was made to correct for plate effects by adjusting observed arrival times by their corresponding residuals from the Amchitka explosions. A significant reduction in the standard error of an observation was achieved.

An obvious next step is to incorporate the plate model in the hypocenter solution using seismic ray tracing in the manner described by Engdahl[1]. In Fig. 1.2 the thirty-nine events have been relocated using a relatively simple plate representation which incorporates a 7 per cent increase in velocity within the plate over the surrounding Herrin mantle. The approximate grid size for this model was 5 X 5 km. The

HERRIN SPHERICALLY SYMMETRIC MODEL

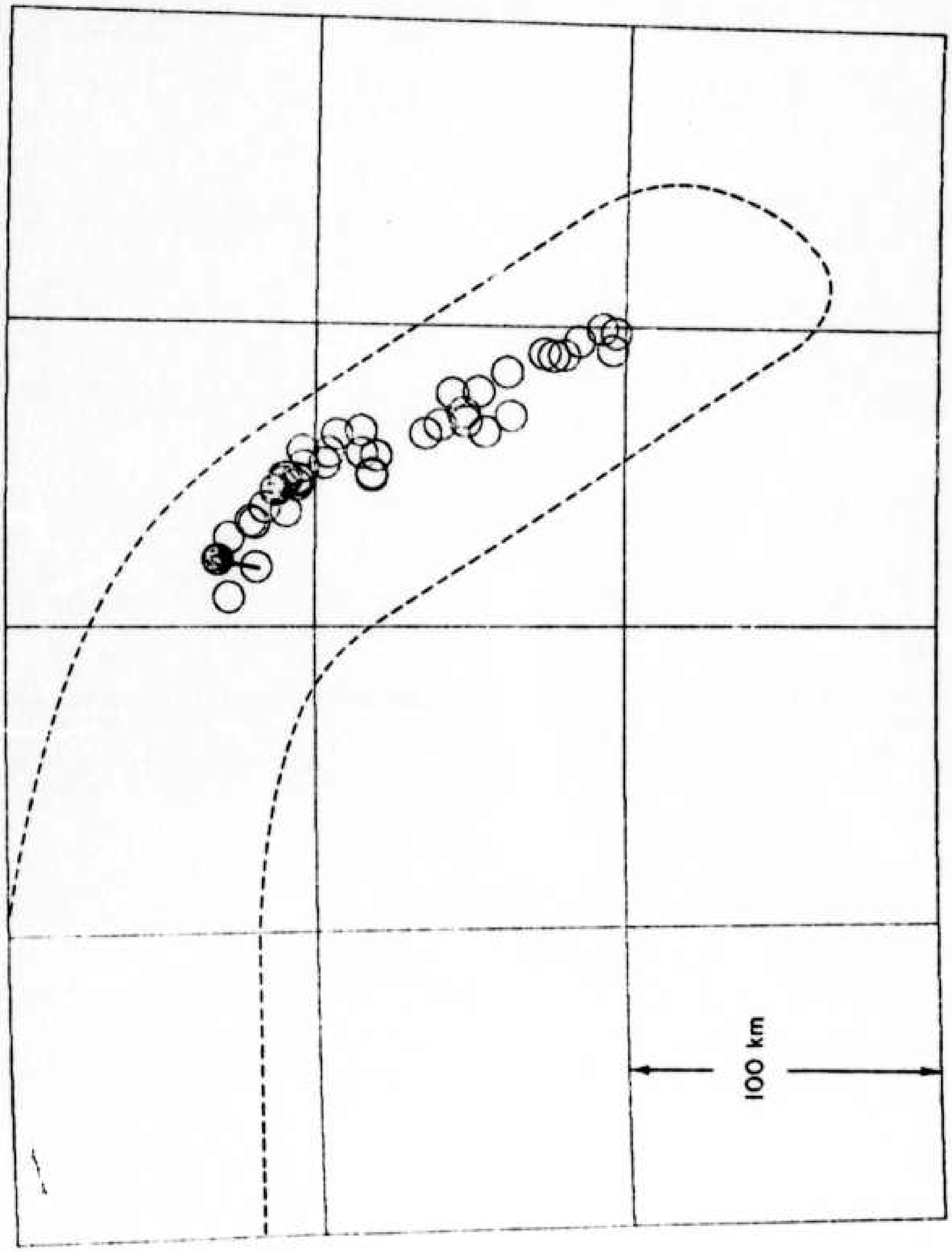


Figure 1.1

HERRIN AMCHITKA PLATE MODEL WITH 7 PERCENT INCREASE

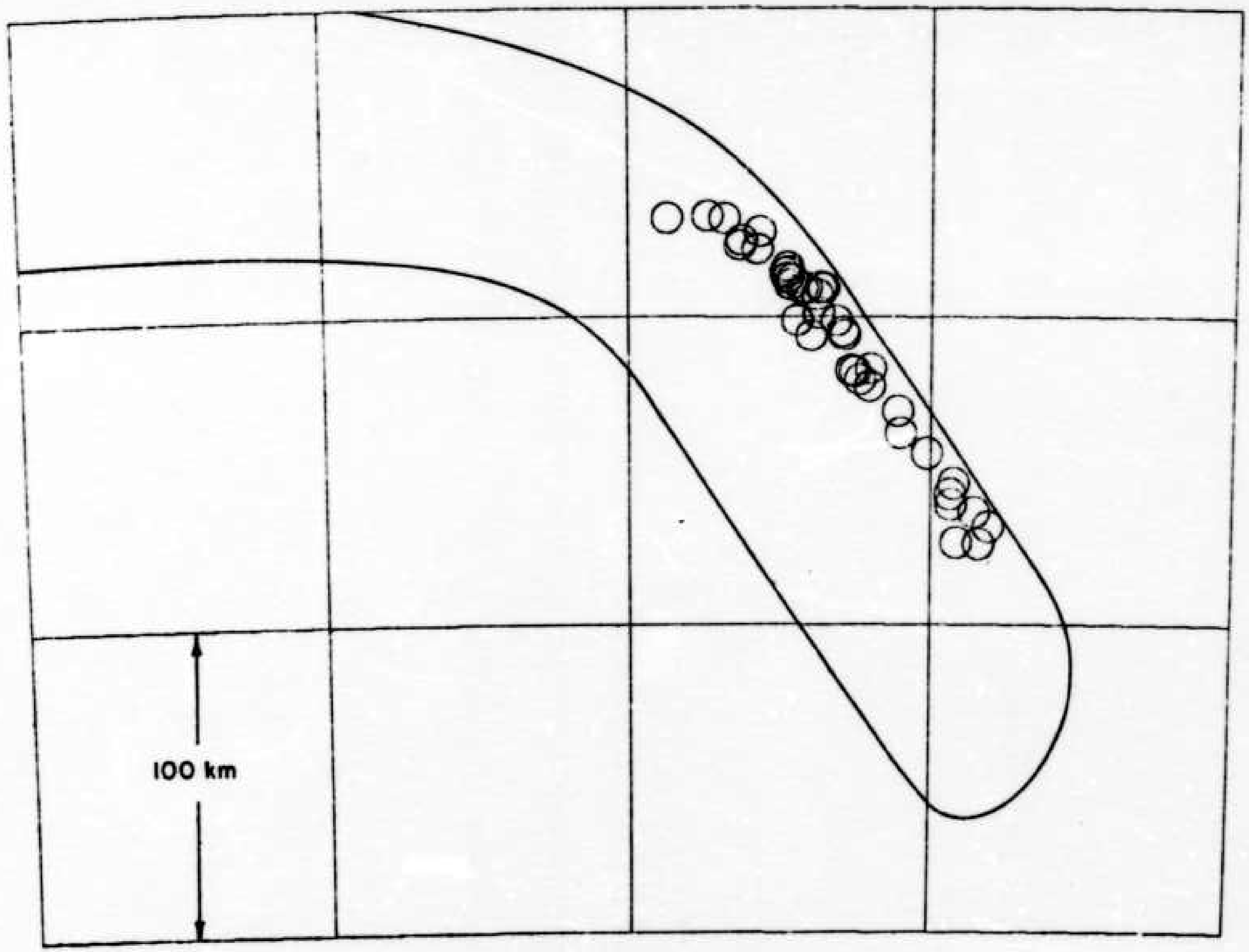


Figure 1.2

effect on the hypocenters is dramatic. They are now concentrated in a rather thin zone (~ 10 km) in the upper half of the plate which also corresponds to the colder, more brittle region of the slab suggested by thermal anomalies[3].

A more realistic velocity model may also be constructed from numerically calculated thermal models of slabs. In Fig. 1.3 is shown a plate model (on a 10 X 10 km grid) derived by perturbing the Herrin velocities with a thermal model of the Aleutian plate derived by Sleep[3]. Hypocenters relocated using the local network and this model again define a thin zone in the colder upper half of the plate, but also corresponding to the region of largest velocity (or thermal) gradient. The solid circles are the same events shown in Fig. 1.1, except relocated by seismic ray tracing using this model. In this case, station corrections applied to the observed arrival times were the residuals obtained from the Amchitka explosions by tracing through this model. The locations of these two events shown in Figs. 1.1 and 1.3 are in close agreement. This is to be expected if the plate structure is a good first approximation to the real Earth.

The teleseismic events shown in Figs. 1.1 and 1.3 also provide a good opportunity to study plate effects on focal mechanisms and $dT/d\Delta$ measurements beyond $30^{\circ}$. Figs. 1.4 and 1.5 are comparisons of ray projections on the lower half of the focal sphere (equal-area azimuthal) for the spherically symmetric and laterally varying Earth models. Only

HERRIN AMCHITKA PLATE MODEL FROM THERMAL ANOMALIES

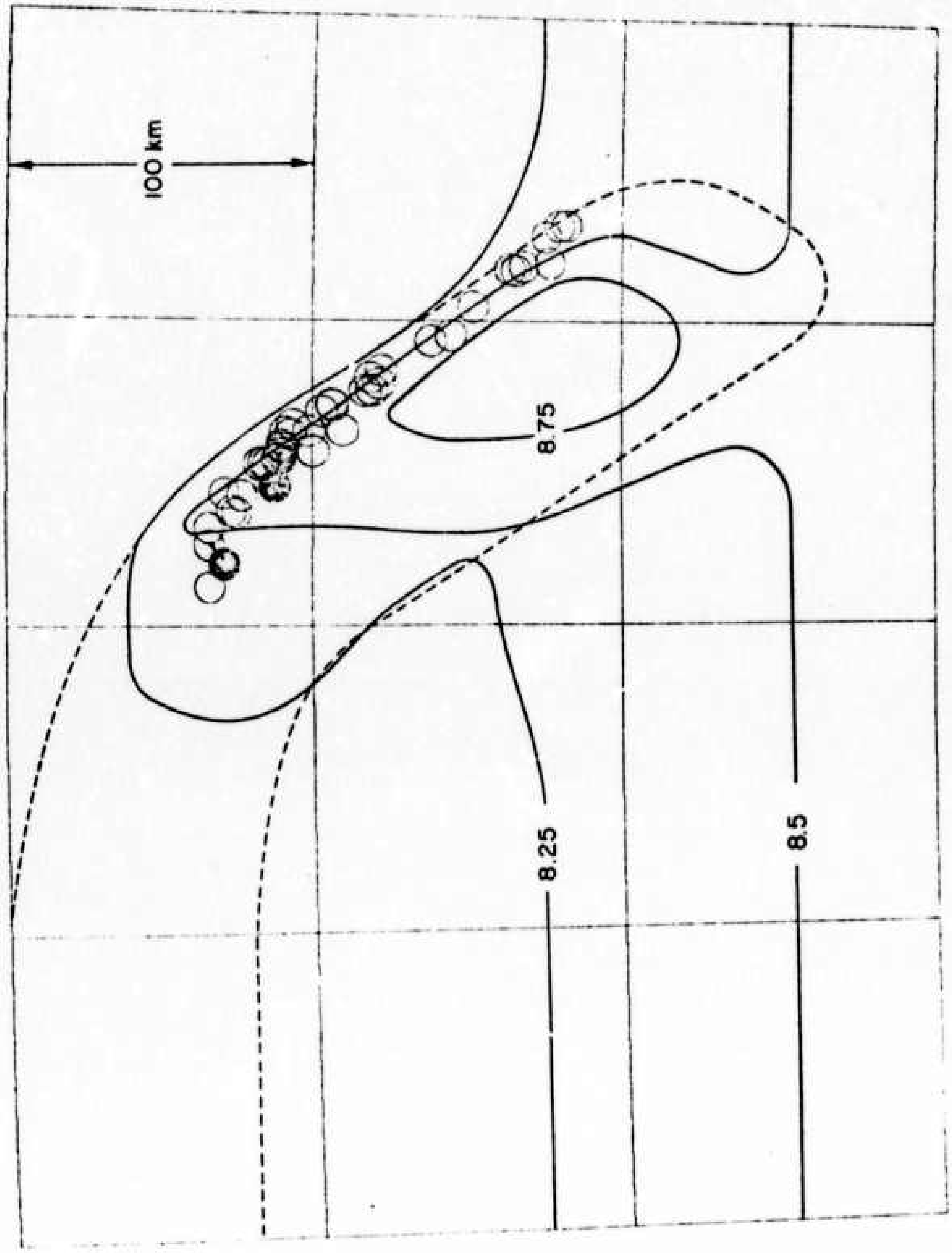


Figure 1.3

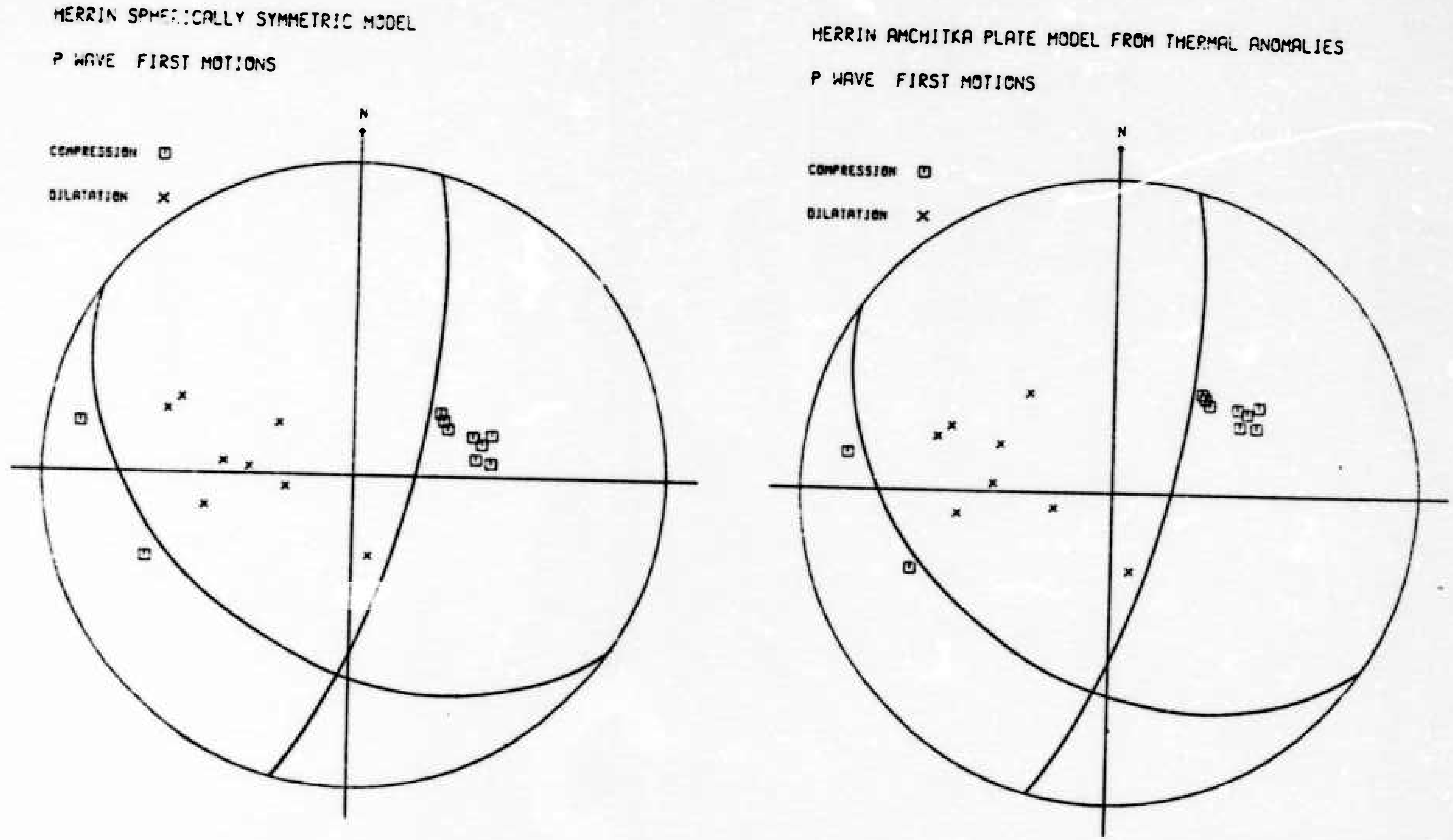
MERRIN SPHERICALLY SYMMETRIC MODEL
P WAVE FIRST MOTIONS
COMPRESSION
DILATATION
N
MERRIN AMCHITKA PLATE MODEL FROM THERMAL ANOMALIES
P WAVE FIRST MOTIONS
COMPRESSION
DILATATION
N

Figure 1.4

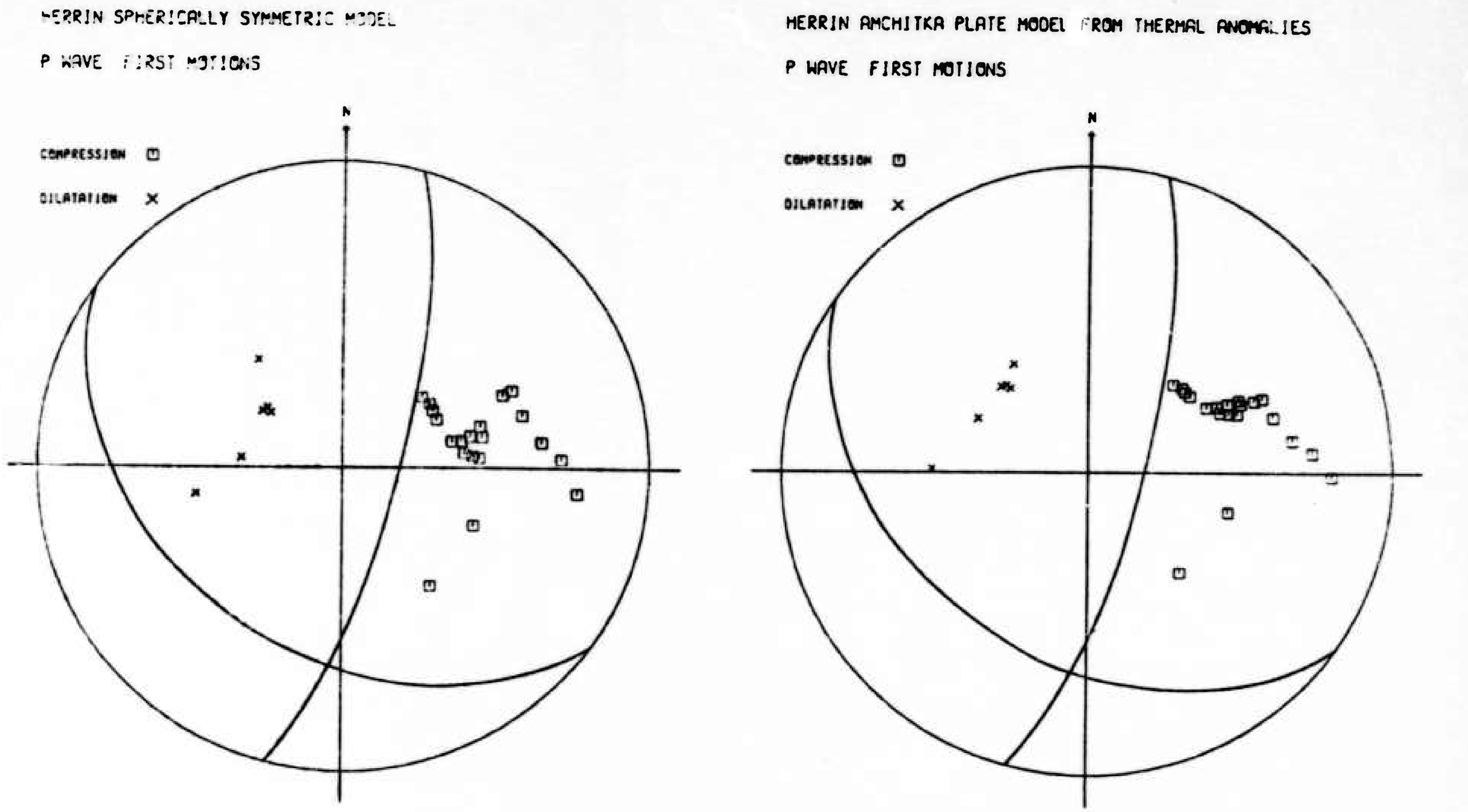
HERRIN SPHERICALLY SYMMETRIC MODEL
P WAVE FIRST MOTIONS
N
COMPRESSION
DILATATION
HERRIN AMCHITKA PLATE MODEL FROM THERMAL ANOMALIES
P WAVE FIRST MOTIONS
N
COMPRESSION
DILATATION

Figure 1.5

data read from WWNSS stations and the Amchitka network by the investigator are shown. Changes in i and $\alpha$ of up to 11° and 20°, respectively, between the two models were computed for rays beyond 30°. The largest changes occurred for rays departing nearly along the strike of the arc. This can be seen in the general counterclockwise rotation of ray points to North America in the NE quadrant. In some instances a rotation of focal angles of this magnitude could produce a corresponding change in the strike of a nearby nodal plane. For these two events the distribution of ray points is such that little or no change in the focal mechanisms is demanded.

The theoretical $dT/d\Delta$ and back azimuth of the wavefront were also computed for stations beyond 30°. The largest departures from a spherically symmetric model were 0.02 sec/° and 0.4°, respectively. This is not a wholly unexpected result since only a small part of the teleseismic path actually sees the laterally varying mantle at the source. This does, however, suggest quantitatively that plate effect will not normally be detectable by seismic arrays at teleseismic distances.

We gratefully acknowledge the cooperation of the National Center for Atmospheric Research in permitting the use of their CDC 7600 computer for the purpose of expediting the development of the computational techniques used in this research.

References.

1. Engdahl, E. R. (1973). Relocation of intermediate depth earthquakes in the Central Aleutians by seismic ray tracing, Nature, Phys. Sci. 245, 23-25.

2. Jacob, K. (1972). Global tectonic implications of anomalous seismic P travel times from the nuclear explosion Longshot, J. Geophys. Res. 77, 2556-2573.

3. Sleep, N. H. (1973). Teleseismic P- wave transmission through slabs. Bull. Seism. Soc. Am. 63, 1349-1373.

## 2. Station Corrections for Soviet Stations

E. R. Engdahl and R. Agrawal

Approximately 4000 residuals of teleseismic P waves reported by stations in the Soviet bulletins for earthquakes deeper then 300 km during 1970-1973 were examined for source-station anomalies. Residuals were first separated into source regions by station to determine if mean residuals vary with the body-wave magnitude of the earthquake (or equivalently, the number of stations reporting) or the depth for each source region. No obvious effects were observed in the plotted data, at least in part because the Soviet bulletins are selective only of the larger magnitude earthquakes.

Station quality appears to vary roughly with reported station sensitivities. Stations reporting to 0.1 sec were not always as reliable as those reporting to 0.5 sec. One station (MAG) shows an abrupt change of mean residual of about 3 sec. during April, 1971, an effect that could be due to an unreported change of location.

Source biases introduced by different source regions were removed by computing station residuals relative to a reliable base station (TLG). These relative residuals had means consistent within a standard error of 0.1 sec. The mean residual was then computed over all source regions for the base station and the relative station means (to the base station) adjusted accordingly to obtain absolute station corrections relative to the Jeffreys-Bullen tables. The results are plotted in Fig. 2.1.

The bracketed numbers in Fig. 2.1 are mean station corrections independently determined by Kogan[1] from Eniwetok explosions and

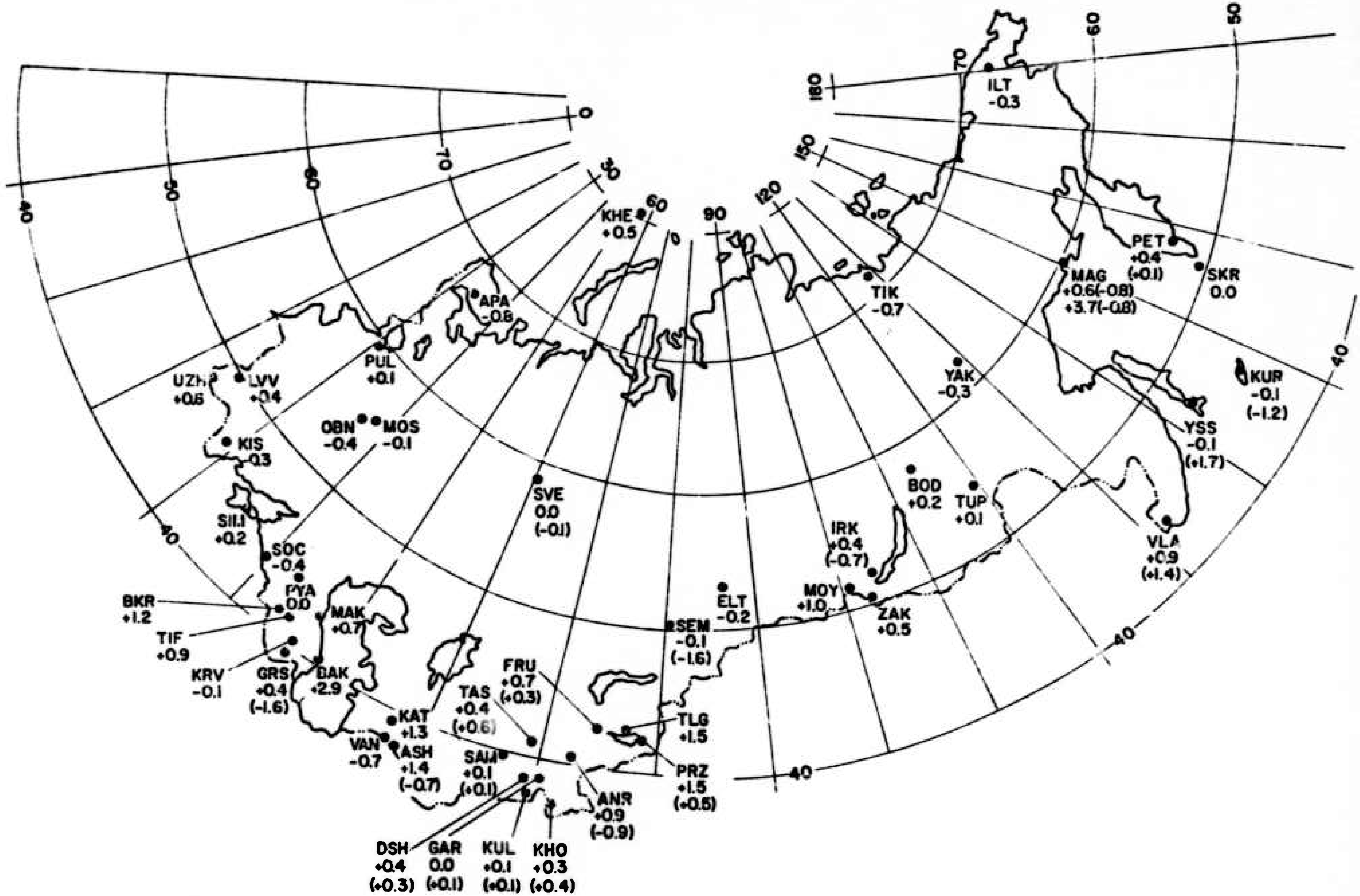
ILT
-0.3
PET
+0.4
(+0.1)
SKR
0.0
MAG
+0.6(-0.8)
+3.7(-0.8)
TIK
-0.7
YAK
-0.3
KUR
-0.1
(-1.2)
YSS
-0.1
(+1.7)
BOD
+0.2
TUP
+0.1
VLA
+0.9
(+1.4)
IRK
+0.4
(-0.7)
MOY
+1.0
ZAK
+0.5
ELT
-0.2
SEM
-0.1
(-1.6)
KHE
+0.5
APA
-0.8
PUL
+0.1
UZHP
+0.6
LVV
+0.4
OBN
-0.4
MOS
-0.1
KIS
0.3
SVE
0.0
(-0.1)
SII.1
+0.2
SOC
-0.4
PYA
0.0
BKR
+1.2
MAK
+0.7
TIF
+0.9
KRV
-0.1
GRS
+0.4
(-1.6)
DAK
+2.9
FRU
+0.7
(+0.3)
TAS
+0.4
(+0.6)
TLG
+1.5
KAT
+1.3
VAN
-0.7
ASH
+1.4
(-0.7)
SAM
+0.1
(+0.1)
PRZ
+1.5
(+0.5)
ANR
+0.9
(-0.9)
DSH
+0.4
(+0.3)
GAR
0.0
(+0.1)
KUL
+0.1
(+0.1)
KHO
+0.3
(+0.4)
0
30
60
90
120
150
180
70
60
50
40

Figure 2. 1

adjusted by +2.0 sec. to the J-B tables. Although these are small samples, they represent high-quality data and are in fair agreement with the results of the deep-earthquake study. In the region north of the Hindu Kush the agreement is to within 0.2 sec.

This study demonstrates the usefulness of the technique, and plans are being made to extend the results to other Asian stations using ISC data from 1964-1970. The station corrections will then provide a means of separating out purely source effects from observations of earthquakes in the Hindu Kush and Kurile-Kamchatka regions.

Reference.

1. Kogan, S. D. (1960). Travel times of longitudinal and transverse waves, calculated from data on nuclear explosions made in the region of the Marshall Islands, Izv., Geophys. Ser., 371-380.

## 3. Depth Determination from Long Period Body Wave Spectra

G. Boucher

The determination of the depth of focus of earthquakes is one of the classical problems in seismology. Although the problem may be regarded as solved in principle, through use of body-wave travel times, depth phases, surface wave amplitudes and spectra, and so forth, well-known practical difficulties remain, particularly in the case of shallow earthquakes. In this research Fourier spectra of body waves recorded on standard WWSSN long period seismograms are interpreted in terms of the spectral modulations produced by the interference of near-source surface reflections and the direct body wave, such as pP and P. The method of analysis has practical value not only in determination of depth of focus (which may be useful in deciding whether a suspicious event might be an explosion or an earthquake), but also in determination of the focal mechanism. This work was intended to lay the groundwork for applying the process to digital seismograms from the High Gain Long Period Network (HGLP). It has been found that a relatively simple model of a body wave phase and one or more near-source surface reflections produces credible and consistent results in some cases, when the precise timing of the depth phase would normally be in doubt. Considerable attention has been given to maximization of the chances for success of the method and to the sources of ambiguity and difficulty.

Focal depth determination by means of long period body waves complements other methods of focal depth determination. When only

teleseismic data are available to define the source parameters of an earthquake, unless the depth of focus is great enough to produce unambiguous depth phases, determination of focal depth is limited to indirect means. Basically this is because of the trade-off between focal depth and origin time in teleseismic location algorithms. Tsai and Aki[1] applied a theory of Saito[2] to determination of focal parameters using surface wave spectra, but the results are not without ambiguity, and either multipath effects or multiple events at the same source may give misleading results. The problem in separating depth-diagnostic phases such as pP from P for shallow earthquakes is that the seismic signals are too close together in time to be distinguished. With short period seismograms the problem is that the complicated structure of the earth results in a body wave signal that lasts for several tens of seconds. Because of the narrow bandwidth of typical instruments it is difficult to pick later arrivals from the nearly sinusoidal signal. On long period records, such as the WWSSN long period instruments, the time resolution is relatively poor, and the signals are somewhat smeared out in time because of the amplitude and phase response characteristics of the instruments, although the signals do not appear so complex. Thus even if it is apparent that a mixture of phases is present in a packet of body waves, it is quite another matter to identify their arrival times and relative senses with certainty. It has been learned in this study that the application of Fourier spectrum techniques to long period body-waves of earthquakes shallower than about 50 km makes the focal depth

problem tractable. Part of the following discussion will be devoted to exploring the liberties that may be taken with mathematical rigor and physical reality in order to achieve useful results.

After treatment of the simple theory, a few examples will be shown to demonstrate the expected modulations on the body-wave spectrum. A second approach will be a comparison of real seismograms with synthetic seismograms made by convolving theoretical seismic pulses and their echoes with the instrument response. The focal depth and corner frequency may be determined simultaneously by visual trial and error, without recourse to Fourier analysis.

Theory.

An easy way to conceptualize the use of spectrum modulations to characterize secondary arrivals is to consider the convolution of a signal, say an elementary P wave, with a pair of impulses which may or may not be mutually reversed in sense. It will be assumed that for practical purposes the signals to be separated are similar in shape, but with possibly different amplitudes. The amplitude spectrum of a pair of identical impulses is a sinusoidal curve with either a maximum or a minimum at zero frequency, depending upon whether the impulses are of the same or opposite sense, respectively. In the general case where the relative amplitude of the second signal is $\pm$ a, and the Fourier amplitude spectrum of the common pulse is f ($\omega$), where $\omega$ is angular frequency, then the modulated Fourier spectrum due to the interference of the second arrival

is $f(\omega) \cdot (1 + a^2 \pm 2a \cos(\omega\tau))$ where $\tau$ is the time interval between events[3,4]. If the two arrivals are dissimilar the situation in the frequency domain becomes much more complicated. For moderate earthquakes such as those studied here the source dimensions are small enough that the separate pulse arrivals may be regarded as similar for practical purposes.

The utility of the method is aided by the form of the elementary source spectrum of the earthquake. Common to dislocation models of the earthquake source function is an essentially flat spectrum from some 'corner frequency' down to zero frequency[5,6]. Thus modulations due to interference predominate over expected peculiarities of the source mechanism as long as the frequency range of interest is below the corner frequency. Because of the shape of the instrument response, noise, and a technical difficulty pointed out by <u>Linde and Sacks</u>[7], it is difficult to establish the very low frequency points of the spectrum. On the other hand, at sufficiently high frequencies attenuation and the effects of the crustal response become severe. Thus there is a region of the spectrum where the frequencies are neither too high or too low, where path and multiple phase effects predominate. One goal of this study was to determine the region of the spectrum where this is true for shallow events of moderate size as recorded by WWSSN long period seismographs.

In the case of long-period seismograms, a recorded body-wave, often can be represented by the convolution of the instrument response

with a rather simple pulse shape of short duration. That is, the effect of layering or other inhomogeneities along the propagation path is sometimes negligible, so that the effect of removing the instrument response is to reproduce essentially the form of the seismic pulse. Thus it may be effective to remove the instrument response from the complex Fourier spectrum of the signal. The reason for this is that the smearing-out of the seismic signal by the instrument response is then eliminated, and seismic pulses of short duration can actually be 'read' from the deconvolved seismogram of direct ground motion. This is usually less satisfactory than looking at the spectrum to determine delay and sense of multiples of a pulse, but it is instructive in other ways since the phase information is utilized, giving a more complete picture. It can also be diagnostic of cases where the simple theory is inadequate, particularly when extra pulses are present.

Although problems of noise and multiple events are discussed in the sections on experimental results, a few comments on the practical aspects of using Fourier transforms for non-stationary signals in the presence of noise may be in order. The essential point is that a seismic body wave signal or phase is finite in duration. On a raw digitized seismogram, if the duration of a source pulse is only a few seconds, then a data sample no longer than 20 or 30 seconds, which is about the length of the most important part of the impulse response of the seismograph system, may be adequate. To take a longer sample is simply

to include other possible phases, and more significantly to include a greater proportion of noise energy. It is obvious, of course, that the sample must be long enough to include a sufficient sample of all the pulses of interest. For example, a sample that includes an adequate length of P, but only the beginning of pP will be modulated correctly in the upper frequency range, but the bottom end of the spectrum will be incorrect, and the vital first hole may be missing. But inclusion of unwanted phases produces unwanted modulation of the spectrum, making interpretation difficult. Since microseismic noise is of a quasi-stationary character the noise power in the spectrum is nearly proportional to record length. For signal-to-noise ratios of the order of 10, as is the case for earthquakes in the size range studied here, any unnecessary amount of noise is intolerable. For isolated signals signal-to-noise ratio is a decreasing function of sample length beyond some point. This is in contrast to the situation for stationary signals and noise where the signal to noise ratio doesn't vary much with sample length, and where it may be possible to characterize the noise well by developing a statistically better determined average. In the case of seismograms, the noise may not be stationary, and no certain advantage accrues from studying noise samples that are longer than adequate signal samples. This is especially true when the record contains noise transients or interfering phases, as often turns out to be the case. It is critical to bear in mind that the travel-time curve of any particular phase may be complicated in certain distance ranges, with duplication or triplication, cusps and other phenomena.

some of which may not be understood. For this reason the interpretation of an earthquake involves numerous lines of evidence, including as many phases as possible and as many stations at different distances as may be necessary.

With reference to the problem of discrimination of underground nuclear explosions, it should be noted that in the case of P waves and other waves of the P type, there will be very little energy at long periods, because of the cancellation effect of the near-source surface reflection of the P type. Thus, an interesting special case, to be discussed in Section 4, is that, in which no detectable long period signal is present.

Experimental Data and Observations.

Data for the numerical experiments were obtained by digitization of photographic enlargements made from WWSSN film chips, using a Calma digitizer. The digitizer is claimed to have accuracy of 0.003 inch; the principal limitation upon the accuracy of the digitization is the steadiness of the operator. The digitizing rate was always at least 1 sample per second of record time, and usually 4 per second. Aliasing effects appear to be negligible. Below 0.5 Hz the spectra for records digitized at 4 samples per second were not significantly difficult in the spectrum below 0.5 Hz from those with a sampling rate of 1 per second. The Fast Fourier Transform algorithm was used to compute Fourier spectra, using either 128 or 512 points, and filling in with zeroes if the sample was shorter than the specified number of transformed points.

This study was based on earthquakes located in the central Aleutian Islands, principally because data from the Aleutian Island Seismic Network helped to insure that the depths obtained from teleseismic solutions are fairly accurate. In this way the technique of depth determination from long period body waves can be evaluated. Data from stations as near as 21 degrees (COL) and as far as 90 degrees (SJG) were used. Magnitudes of events were in the range 5.5 to 6 as determined by the National Earthquake Information Service of the U.S. Geological Survey. The depths given in the Preliminary Determination of Epicenters were used as a guide in preliminary selection of data. It is mainly by comparison with the depths determined by the PDE program that the method is justified for use in other areas where depth control is poorer.

TABLE I

| Event | Lat. | Long. | Depth,km | $m_b/M_s$ | Location | Figure # |
|---|---|---|---|---|---|---|
| 05-14-69<br>19 32 54.2 | 51.3N | 179.2W | 21 | 6.2/7.0 | Andreanof Is. | 1. |
| 09-12-69<br>08 57 07.3 | 51.2N | 179.2W | 48 | 6.0/6.6 | " | 2. |
| 07-18-70<br>01 48 38.9 | 51.4N | 178.5W | 46 | 5.7/5.9 | " | 3. |
| 08-04-69<br>17 19 19.6 | 5.7S | 125.3E | 521 | $m_b$=6.2 | Banda Sea | 5. |
| 08-30-70<br>17 46 09.0 | 52.4N | 151.6E | 645 | $m_b$-6.6 | Sea of Okhotsk | 6. |

Parameters for the earthquakes treated in this report are given in Table I. The main emphasis is upon two groups of earthquakes, rather shallow (20-25 km) and somewhat deeper(40-60 km). Brief mention will be made of a deep focus event, not to study pP, but to illustrate some apparent source mechanism effects that are susceptible to the same sort of analysis.

The theory of detecting pP-P or sP-P intervals from modulations of the spectrum is straightforward, but typical spectrums made from seismograms have modulations from other causes that must be sorted out before the correct ones can be identified. The spectrum will have irregularities due to background noise, effects of the transmission path that were neglected in the theory, and perhaps unsuspected multiplicity of the source. The sP phase is also of primary importance. The focal mechanism of the earthquake, which affects both the relative amplitude and sense of the phases being examined, adds another set of variables that affect each seismogram differently. The solution to the problem of finding the correct set of modulations is to use a set of different sample lengths and time windows for each recorded phase (chosen logically from the original seismogram, of course), and to compare observations among a number of recordings from different stations. If available, a nearby event can serve as a control. The first technique eliminates spurious modulations that arise somehow from the choice of sample length, for example when an undesired phase is included within the sample. The second, to use a specific example, exploits the small but measurable

variation of pP-P interval with epicentral distance as predicted by the travel time tables. Clearly a hypothetical choice of a particular spectral modulation that is not only stable with respect to sampling length, but also shows the proper behavior as a function of epicentral distance is likely to be the correct one. A satisfying exercise, in fact, is to vary the length of the sampling window about an appropriate phase in order to deliberately include an unwanted phase. As the window length is extended to include the intruding phase, the effect of that phase can be seen to develop in the spectra. This serves as encouragement that the technique is basically correct. It also shows that, as long as one does not stray from the frequency range where the data are reliable, the sampling problem is not too severe,and it is possible to use rather subjective criteria to determine just what constitutes the wave packet of interest, and what should be rejected. One reason this point must be emphasized is that for the earthquakes of primary interest, the signal to noise ratios are typically rather low. The second is that, for earthquakes in the upper end of the magnitude range studied, i.e. greater than 6.0, the likelihood that the event will be a multiple one is considerable. That situation must be identified by inspection of several seismograms or else from indications given by the spectra. It is necessary to look at records from several stations and from several different phases, if possible, to resolve the usual ambiguities that are seen.

The first example considered is the rather complicated earthquake of May 14, 1969. The whole suite of spectrum data obtained are

shown, in order to provide a complete picture of the interpretive process. Other examples will then be discussed in less detail, representing presumably less complex situations: Figure 3.1 shows the entire suite of data from stations COL (P), KIP (P, PP) GOL (P), and SJG (P). The letters in parentheses here signify the phase which together with its surface reflection, was used in the interpretation; e.g. (P) means the pP-P (or possibly sP-P) time interval was determined. Figures 3.2 and 3.3 illustrate other examples as described in the figure captions.

It is sometimes unavoidable to include unwanted phase arrivals within the time window used to determine the spectrum. Since the sP phase is likely to be present in addition to pP, for example, the spectrum is sometimes modulated by more than 1 sinusoid. Interpretation by inspection of a sum of sinusoids of mixed phase and different amplitudes is difficult, so that a useful approach is to model various interpretations by a sequence of impulses in the time domain, which are readily converted to spectra for comparison. Since the instrument response and the source spectrum in the period range of 10 to 100 seconds are reasonably flat, it does not introduce much error to approximate phase arrivals by spikes for moderately large earthquakes, the main proviso being that the corner frequency is above the frequency range of interest.

Inasmuch as a some subjective analysis turns out to be required in most cases in the interpretation of spectra, and since the original seismograms are the primary resource on which to base the subjective analysis, an alternative method of determining depth of focus suggests

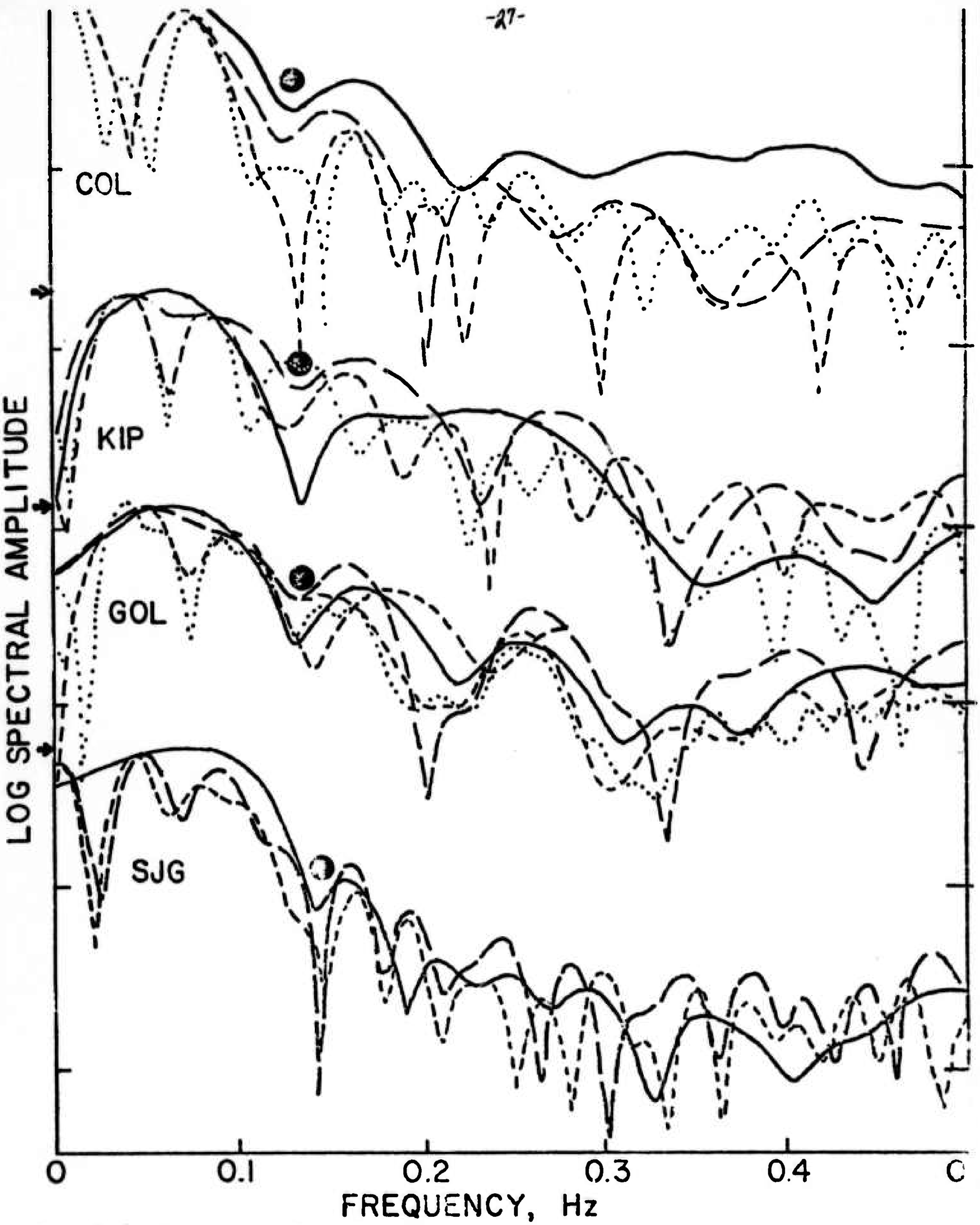


Fig. 3.1. Earthquake of May 14, 1969. Spectra of teleseismic P waves with different sample lengths to show the existence of a stable minimum (dot) at 0.133-0.141 Hz, signifying a pP - P time between 7.1 and 7.5 sec. COL = College, Alaska; KIP = Kipapa, Hawaii; GOL = Golden, Colorado; SJG = San Juan, Puerto Rico. The choice of pP-P time is also based upon additional phases not shown here, such as pPP-PP and sS-S. Spectra are normalized to maximum apmlitude, shown by arrows. Different lines are different sample lengths. No instrument response correction.

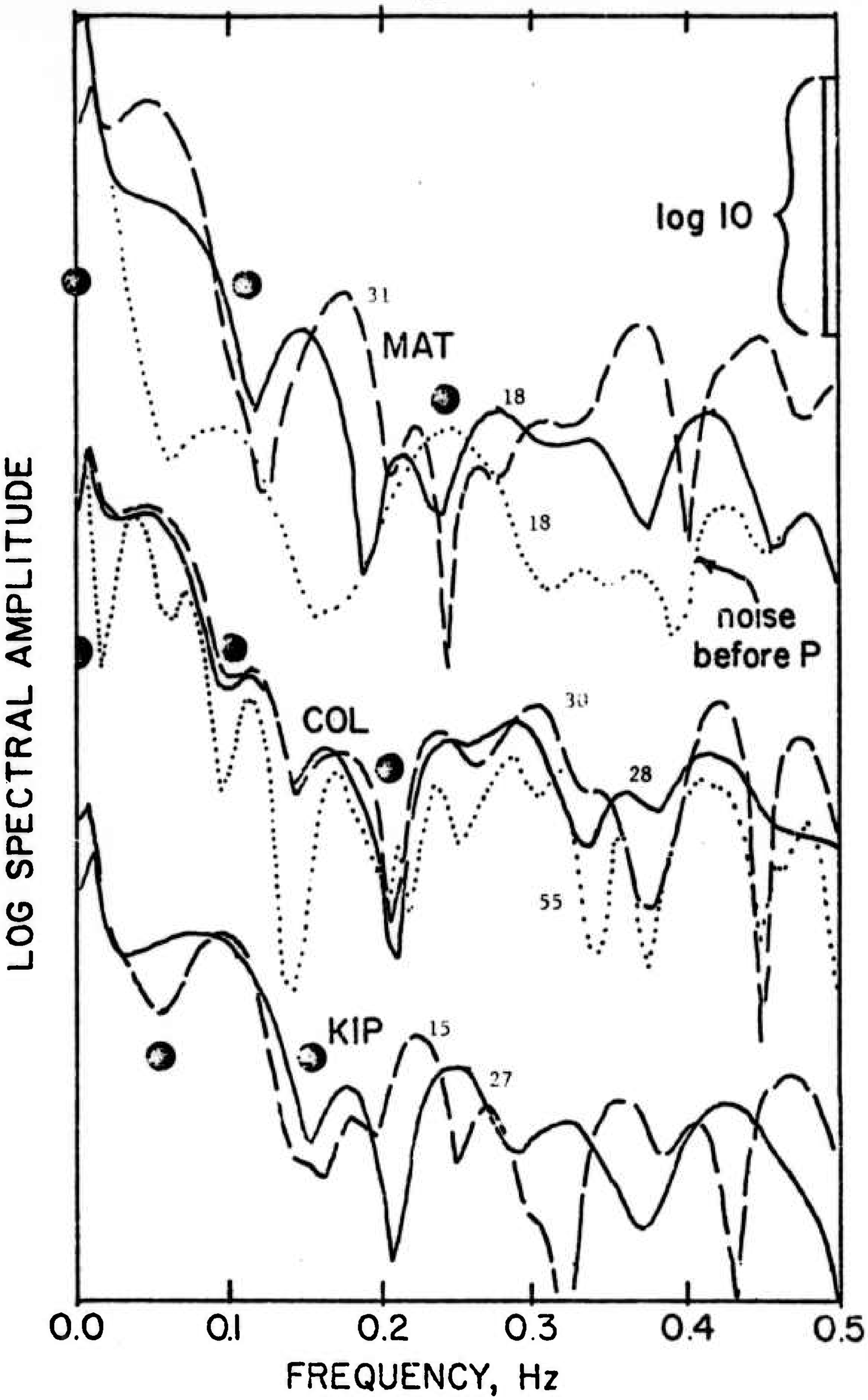


Fig. 3.2. Earthquake of Sept. 12, 1969. Spectra of P waves showing pP out of phase with P at Matushiro (MAT) and College (COL), and in phase at Kipapa (KIP). The numbers give sample lengths in seconds. The short sample at KIP was inadequate to develop the low frequency hole corresponding to the first minimum. The pP-P time estimated from these and other data is 9.5-10 sec.

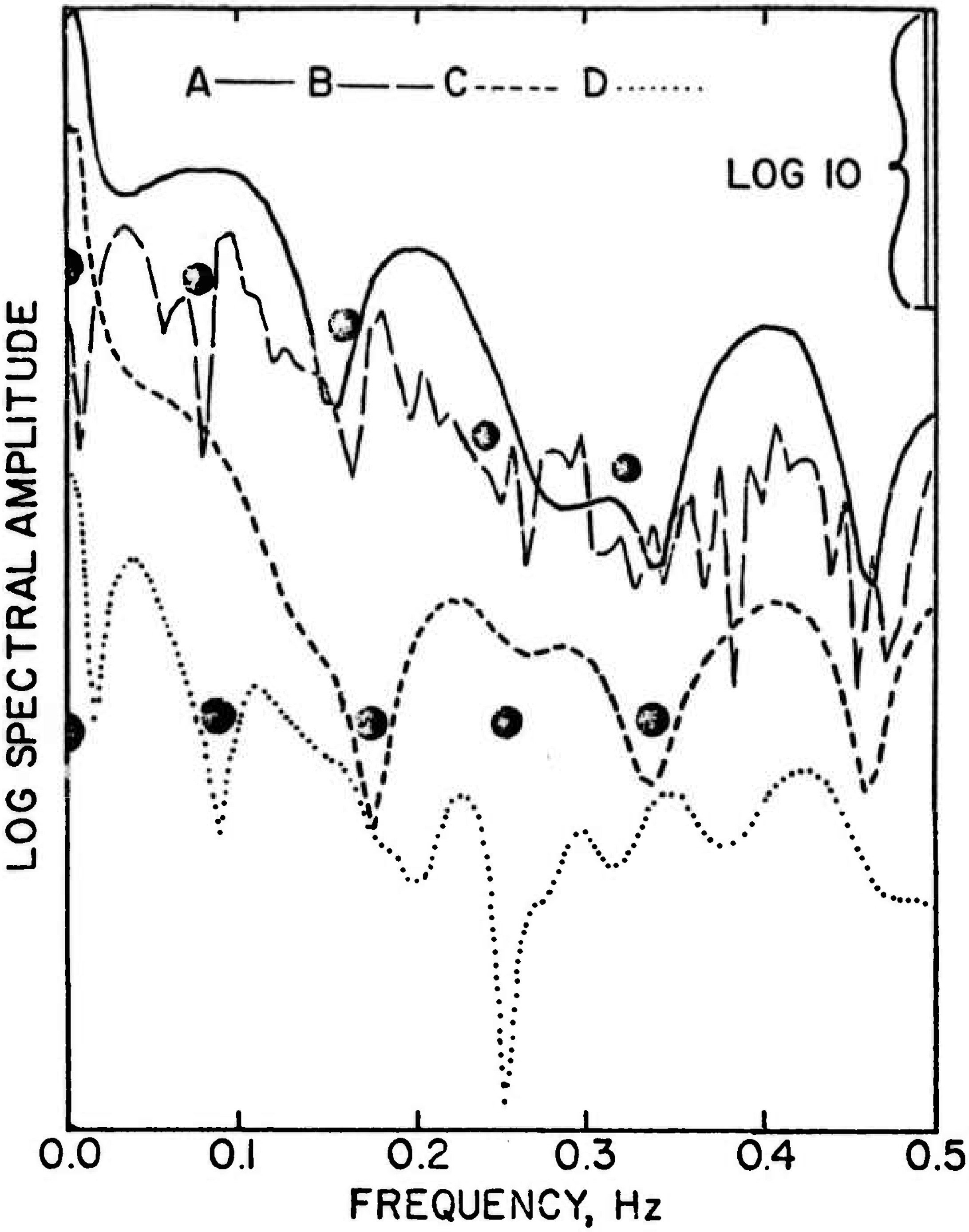


Fig. 3.3. Earthquake of July 18, 1970. Teleseismic P-wave spectra. A and B are from the Golden, Colorado record. Sample lengths are 13 and 67 sec, respectively. C and D are from the College, Alaska, record. Sample lengths are 18 and 43 sec, respectively. This earthquake was located by the National Earthquake Information Center at 43 km depth. The sample length in the short samples was inadequate to display any but 1 of the minima associated with the probable pP-P time, which is rather well determined at 11.3 sec from the long sample at College, and 12.7 sec at Golden.

itself. This is to prepare synthetic seismograms based upon different assumptions about the relative size, timing and sense of arrival of phases, using a reasonable model for the pulse shapes to be expected. The sequence of pulses is then convolved with the instrument response and plotted to produce an overlay for direct visual comparison with the seismogram. In practice, it turns out to be convenient and necessary to include the corner frequency of the phase as part of the process, since WWSSN long period instruments also respond to frequencies of the order of 1 Hz, even though at reduced magnification. Thus a rather simple process can be used to determine not only depth of focus but corner frequency in favorable cases. Figure 3.4 shows a representative set of synthetic seismograms for different assumptions using the far-field pulse shape suggested by Brune[6]. For use in other phases of this study, a microfilm plot of several hundred such artifical seismograms was prepared at a very small cost. Clearly it is not possible to cover all possible situations with a finite number of overlay seismograms, but a good estimate of earthquake parameters can be made with a fairly coarse spacing of sample parameters. The time of first zero crossing, the ratio of the overshoot pulse amplitude (second half cycle) to the first half cycle amplitude, and the time of the second zero crossing are the basic parameters used to make an interpretation. Furthermore, anomalous arrivals are sometimes evident at a glance from the comparison. To illustrate the usefulness of the technique, Fig. 3.5 shows

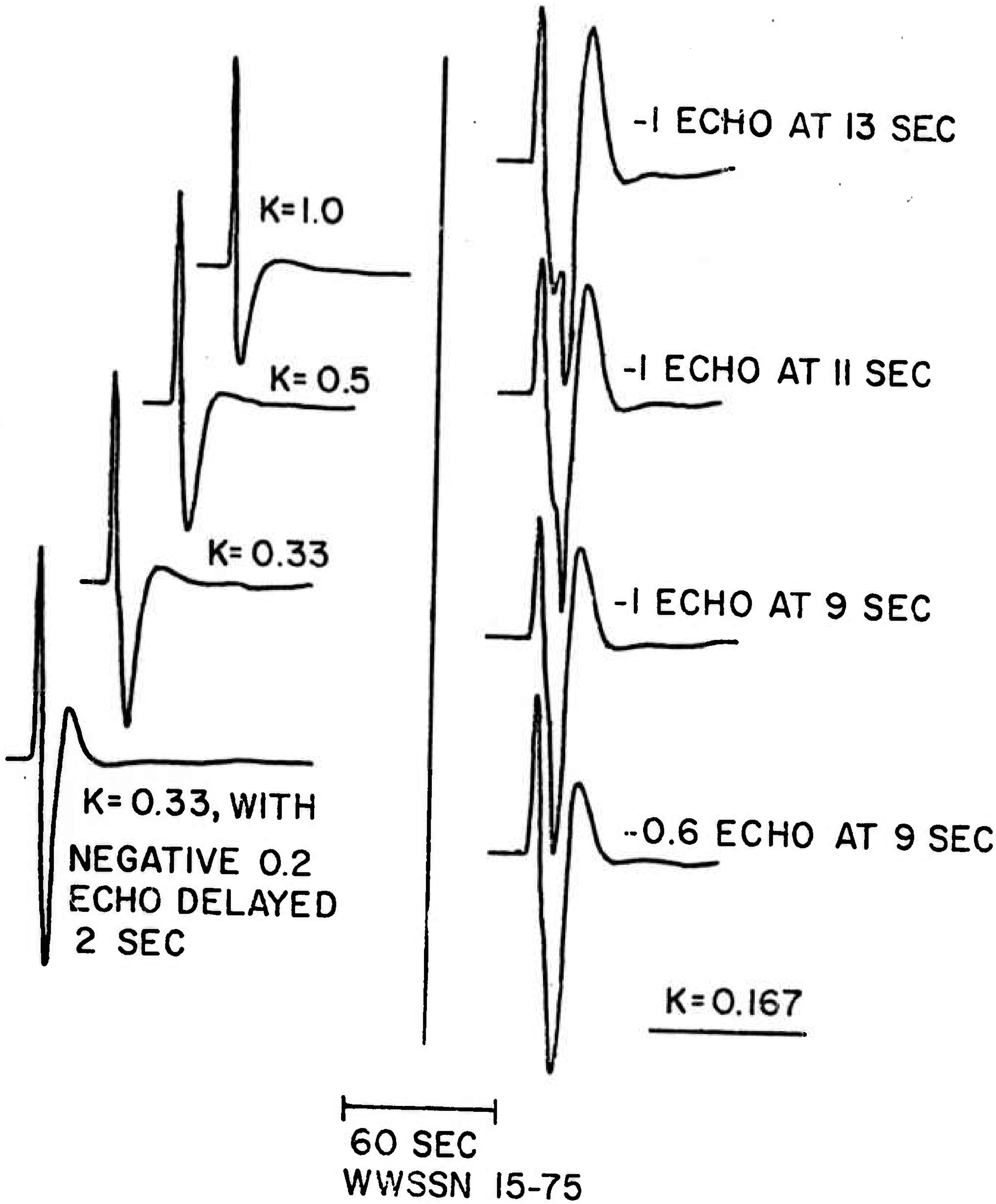


Fig. 3.4. Synthetic seismograms made by convolving the WWSSN LP instrument response with a pulse and its echo ( to represent a reversed pP) for different assumptions about corner frequency, and timing and size of echo. The primary pulse shape is that suggested by Brune (1970) as $f(t) = A\,t\,\exp(-2.27\,Kt)$, and $K$ is roughly proportional to the corner frequency, which is related to the finite source size.

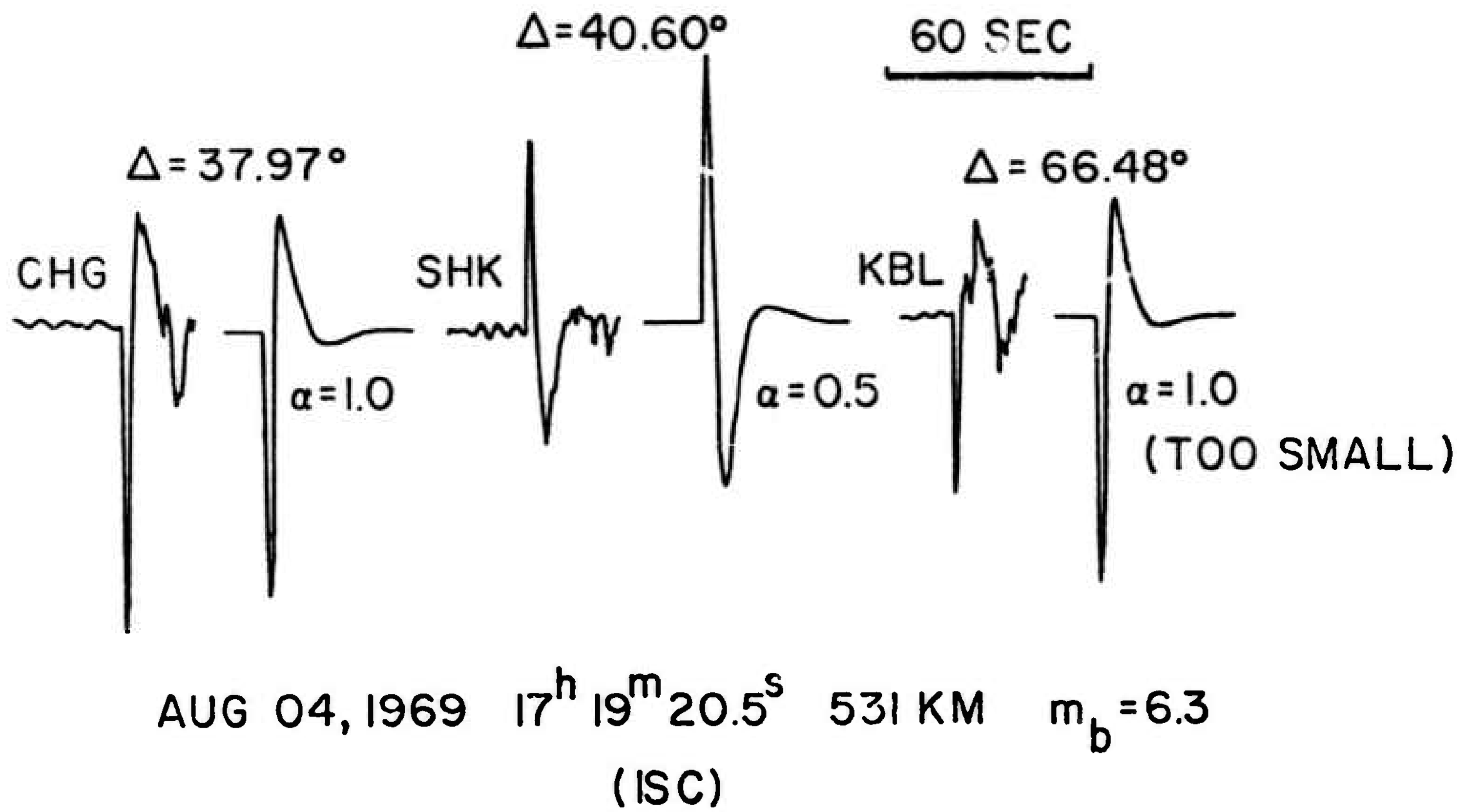


Fig. 3.5. Selected P-waves from the earthquake of Aug. 4, 1969, showing the possibility of fitting synthetic pulses with different corner frequencies. Here α replaces the K in figure 4, and is roughly equal to the reciprocal of the corner frequency. Since this is a deep earthquake (645 km) no surface reflections like pP or sP are included in the sample shown. Most theories predict that the corner frequency will be slightly different in different directions from the source.

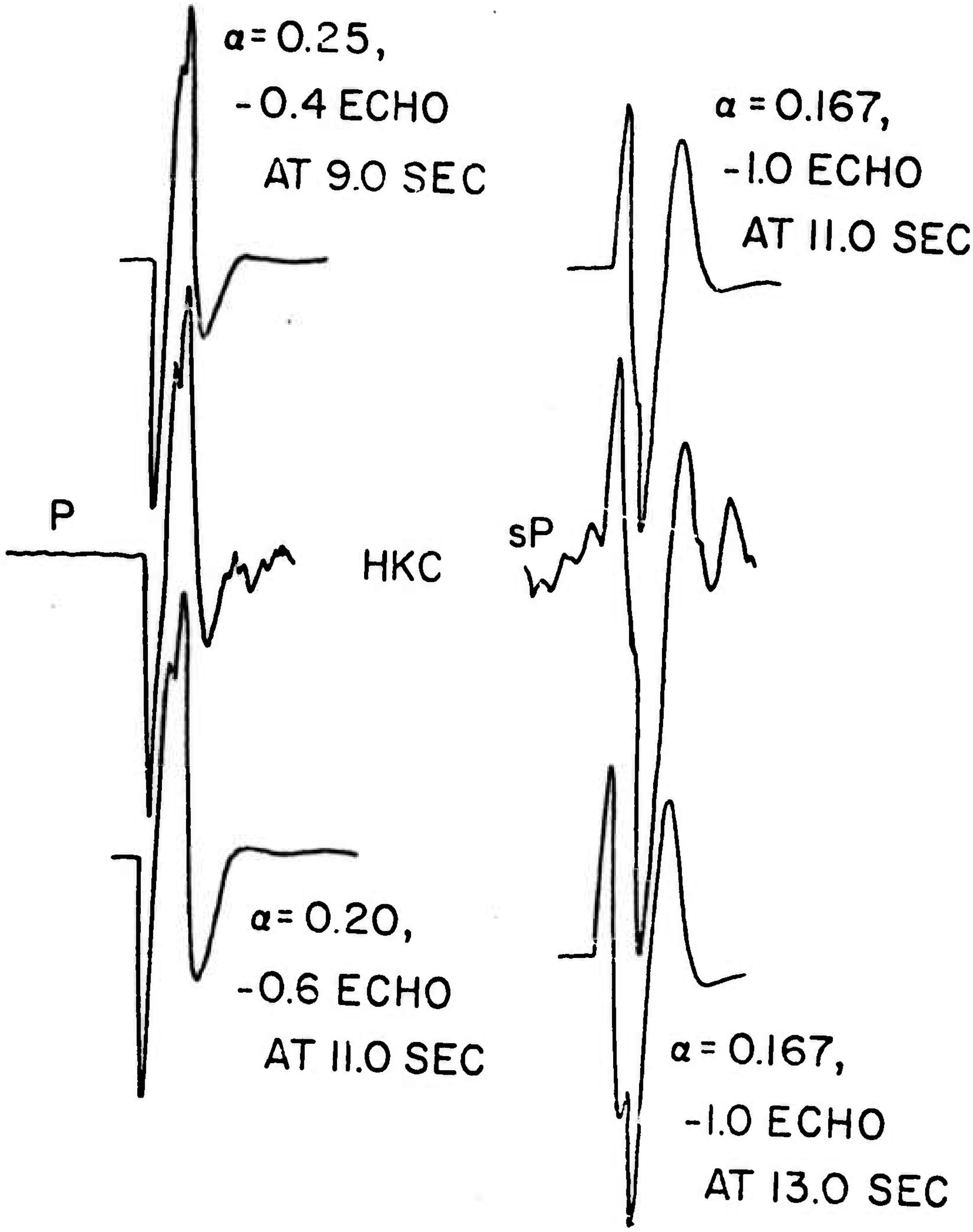


Fig. 3 .6. P wave from the Aug. 30, 1970 earthquake in the Sea of Okhotsk. The LPZ record from Hong Kong (HKC) is shown as an example. On this and other records there appears to be a strong negative phase at about 12 sec after the initial arrival. Comparison among numerous high quality records from this earthquake indicate that this negative event is a source effect and not an effect of the propagation path.

an example of a deep earthquake in the Banda Sea with simple pulse shapes. In a second earthquake, Fig. 3.6, a secondary phase apparently opposite in sign to the initial P phase is observed at about 13 seconds delay. The phase is observed on several stations with consistent timing, so that it does not appear to be a result of some local peculiarity of the travel path. The interpretation of this phase will not be considered here.

Conclusions.

This first conclusion of this study is the general success of the method as applied to standard WWSSN long period seismograms and the determination of its range of applicability. Second is the identification of the sources of probable error, and methods of dealing with them. Third is the recognition of directions in which to seek improvement of the limiting parameters to make the method more generally useful.

The principal conclusion from the study is that, given certain preconditions on the events themselves, it is possible to identify specific modulations in earthquake body-wave spectra obtained from digitized paper records of WWSSN long period instruments. In general it is safe to say that this can be done in the range of frequencies where the signal-to-noise ratio is of the order of 10 or more, where noise must be considered to arise both from the earth-instrument system on the one hand, and from the process of digitization on the other. Taking a conservative but realistic position that the useful frequency range is 0.01 to 0.2 Hz, depth as shallow as 6 or 10 km from sS-S and 10 or 15 km from pP-P,

depending respectively upon whether the surface reflection is in-phase or out-of-phase with the direct wave, can be determined. Absence of any modulation may be useful information, but is not definitive by itself. Sometimes only a single 'hole' can be located within the reliable frequency range. The interpretation of the spectrum may be aided by a determination of the focal mechanism of the earthquake, principally to determine whether zero frequency is expected to be a maximum or a minimum. Conversely, the spectral modulation, if determined well enough, may contribute to determination of the focal mechanism, by indicating the first motion of various phases emerging from the top of the focal sphere. A technique that deals with noise problems about as well as careful analysis of the spectra, and takes advantage of some of the useful integrating properties of the human eye, is to compare a phase on the original seismogram with a synthetic pulse generated from a pulse and suitably timed echo of the proper amplitude. This simple procedure, which by a natural extension includes an estimation of the corner frequency of the event, produces surprisingly good results and might well become a useful part of routine interpretation of seismograms.

The discussion of the sources of probable error will make it apparent why this particular technique has rarely, if ever, been applied in the past. Such problems as microseismic noise, instrument problems (such as spurious transients), and errors in digitizing paper records are well known and have predictable results on the spectrum. More fundamental problems arise from properties of the earthquake source and the earth

itself. The most significant manifestation of the former is the likelihood that an "earthquake" may in fact consist of a number of major events which can be sorted out only by considerable effort. In the present study of shallow to intermediate depth earthquakes in the central Aleutian Islands region, it appears that events with magnitudes ($m_b$) near 6.0 and above are quite likely to exhibit multiplicity, whereas for events of perhaps one-half magnitude less, multiplicity seems much rarer. Of course, if multiplicity is the object of study, spectral interpretation techniques can easily be applied, using appropriate caution. The difficulty presented by the Earth itself as a transmitting medium is obvious from consideration of a single seismogram. From the viewpoint of classical seismology, there are a number of 'arrivals' visible on a seismogram, many of which can be identified on the basis of classical ray theory, or as leaking modes or surface wave modes. Unfortunately every wiggle on every seismogram has not been accounted for in detail, so that there may be uncertainty about the source of some of the complications visible on a spectrum. But even avoiding this particular complication, the presence of other, well known phases on the record near the one of interest means that the time sample used for the Fourier transformation must be of limited length, and it also means that the baseline of the record will be poorly determined. Hence the spectral amplitudes at very low frequencies are not useful as a rule, and a key point in the interpretation is always the presence of a minimum or a maximum at zero frequency. As the time sample is lengthened to include more and more of an undesired phase, the effect

can be seen on the spectrum as an increased degree of modulation of its own which eventually may swamp the modulation that is being sought for interpretation. The practical solution to all of these problems is to compare various types of data. For each record, a proper sample length or range of sample lengths must be chosen, in order to eliminate spurious arrivals and yet have as long a sample of data as is practicable, to improve the reliability of the lower frequency ranges of the spectrum. It is further necessary to use as many different phases as possible, and as many records as may be necessary to make sure the interpretations are consistent and reliable.

Since the motivation for the use of long-period seismograms in the first place was to avoid the complications of the short-period crustal response of the earth, the only useful extension of the usable frequency range to higher frequencies would be in the direction of suppressing the microseismic noise of periods near and just below 10 seconds, since that would allow accurate determination of the spectrums of events of smaller magnitude and lesser depth than is currently the case. Some improvement at the longer period end of the spectrum would presumably result from use of instruments of improved stability at periods greater than 100 seconds, preferably recorded digitally to bypass the hand digitization process. Clearly the better the long period end of the spectrum can be specified, the easier it is to determine whether zero is a maximum or minimum, and the more accurately spectrum modulations can be identified. A case of considerable interest is that of underground explosions. Since nearly

total destructive interference at long periods results from the interference of P and pP, the absence of substantial energy at long periods in the P phase of an event, even at a single station, would be indicative of an explosion or at least an extremely shallow event, although tectonic strain release could of course negate the converse proposition.

References.


1. Tsai, Y-B, and Keiiti Aki, Precise focal depth determination from amplitude spectra of surface waves. Journ. Geophys. Res. 75, 5729-5744.

2. Saito, M., Excitation of free oscillations and surface waves by a point source in a vertically heterogeneous earth, Jour. Geophys. Res. 72, 3689-3699, 1967.

3. Pilant, W. L., and Leon Knopoff, Observations of multiple seismic events, Bull. Seis. Soc. Am. 54, 13-39, 1964.

4. Bracewell, R., The Fourier transform and its applications, McGraw-Hill, New York: 1965.

5. Aki, K., Scaling law of seismic spectrums, Jour. Geophys Res. 72, 1217-1231, 1967.

6. Brune, J. N., Tectonic stress and the spectra of seismic shear waves from earthquakes, Jour. Geophys. Res. 75, 4997, 1970.

7. Linde, A. and S. Sacks, Errors in the spectral analysis of long-period seismic body waves, Jour. Geophys. Res. 76, 3326-3336, 1971.

## 4. Use of HGLP Digital Data for Studies of Body Waves of Earthquakes and Explosions in Central Asia

G. Boucher

The objective of this program is to explore the possibility of applying the spectrum modulation techniques discussed in Section 3, or other techniques that might prove fruitful, to digital data from the High Gain Long period Seismograph Network. This work is currently in progress.

In principle, long period body waves of a seismic event may be expected to contain useful information about source size, focal mechanism, and depth of focus. In practice there is a lower limit to the magnitude of an event for which long period body waves can be observed, and in general this limit is larger than the lower limit of events for which surface waves can be detected, at least for shallow earthquakes. However, because of the potential usefulness of the long period body wave information, it is fruitful to determine the circumstances under which the waves can be observed, then to extract the information that is available. It is necessary to extend the study to the smallest possible events, in the context of the problem of discrimination of underground nuclear explosions, because discrimination in the current state of the art becomes less certain with decreasing magnitude of event. There are two theoretical advantages inherent in the digital data from the HGLP network. First, the instruments have been designed for increased stability in the intermediate and long period range. Second, the digital instruments have wide dynamic range and the data are convenient for various computer manipulations of the

signal, including rotation of coordinates, filtering, and linear as well as non-linear operations in the time and frequency domains.

In the initial stage of this investigation, the approach may be likened to that of the classical seismologist. That is, records from various events and stations are examined to determine the presence and the characteristics of various body phases, and to characterize the background noise. One of the striking differences between the presumed explosions and the small number of earthquakes studied so far is their greatly different excitation of long period energy of various types, using the short-period body wave mgnitude $m_b$ (as determined by the PDE calculations) as the parameter. This is in accord with previous studies, but it is particularly visually striking on HGLP seismograms. For example, an earthquake with $m_b$ given as 6.0 commonly has body wave amplitudes 10 or more times the background noise amplitude and it is simple to move down the record and pick out phase after phase as predicted by the travel time curves. A typical explosion, on the other hand, with $m_b$ given as 6.0, is far less impressive. In particular phases of the P type, including multiples and surface reflections generally cannot be identified at all on the raw records. It is frequently possible, to identify a few phases of the SV type, notably S and PS (or more likely SP) in appropriate distance ranges, but they are almost lost in the noise in most cases, and the multitude of phases predicted by the travel-time curves are generally not discernible. An attempt to quantify this difference will be made; it is considered to be a significant body of information to contribute to the

problem of earthquake - explosion discrimination. The excitation of long period waves of the SV type by explosions is considered rather striking, and will be the subject of a special commentary.

The research program to date has been devoted primarily to analysis of presumed explosions in Central Asia. Earthquakes in the general region have also been studied in order to give a broader framework. This initial emphasis has necessarily directed the bulk of the effort into certain categories, because of the signal amplitude constraints imposed by the existing suite of explosion data. The largest recent explosions within the Soviet Union have been assigned magnitudes ($m_b$) of 6.3 at most. Such explosions produce rather small body waves on the HGLP instruments (with respect to the background noise levels) and so far in this study only surface waves have been observed from explosions with magnitudes as small as 5.0. For this reason the thrust of the analysis has been in the direction of identifying and comparing different wave arrivals in order to establish general familiarity with the character of the seismograms; spectrum analysis and optimized filtering of the records will be the subject of the remainder of the work on the project.

A constraint upon the progress of the research which had been unexpected at its inception has been the relatively small amount of data actually available, compared with the potential amount. Some 15 stations of the HGLP type are now in existence, but the largest number of stations the author has ever seen for a given event has been 7. Usually the number is substantially less than that, and data from some of the stations have

never been seen at all. The situation is improving through the efforts of the Albuquerque Seismological Center, which now has responsibility for operation of most of the network, but their prediction is that a good quality operation is still some time in the future. Instrument malfunctions are rather frequent, and this further limits the comprehensiveness of the analysis.

The first few figures are merely examples of data from specific events. They will show, still using $m_b$ as a descriptor, what can be expected for various sized events, both explosions and earthquakes, at various distances. Table I lists parameters of the events shown, together with pertinent station data. In most cases, the horizontal components have been roughly rotated into radial and transverse components. The transformation is necessarily rough because the frequency responses and nominal magnifications of the NS and EW components at each station are typically different, and in the absence of recent data the reliability of the data that are available is not known. The instruments were treated as if the horizontal components had the same magnification and the same frequency response. Except in one case the results are quite adequate, in terms of separation of Love and Rayleigh waves, and of SH and SV type motion; a detailed normalization procedure using recent calibration data would naturally be preferable. Unfortunately the long-period noise level at all stations in the network is much higher on the horizontal instruments than on the vertical instruments. Evidently this has to do primarily with tilts, as the vertical instruments are relatively unaffected.

## TABLE I

| Date | Origin time | Lat. | Lon. | Depth, km | $m_b/M_S$ | Location |
|---|---|---|---|---|---|---|
| Explosions (presumed) | | | | | | |
| Nov. 2, '72 | 01 26 57.6 | 49.9N | 78.8E | "0" | 6.2 | E. Kazakhstan |
| Dec. 10, '72 | 04 26 57.7 | 49.8N | 78.0E | "0" | 5.7 | " |
| " | " 27 08.4 | 50.1N | 78.8E | "0" | 6.0 (BRK) | " |
| Earthquakes | | | | | | |
| Aug. 31, '72 | 14 03 16.3 | 52.3N | 95.4E | "N" | 5.5/4.9 | RSFSR: Sayan Mt. Region |
| Sep. 4, '72 | 00 14 10.0 | 35.9N | 73.4E | 55 | 5.5 | Tadzhik SSR |
| Sep. 30, '72 | 06 59 59.8 | 36.4N | 70.6E | 204 | 4.9 | Tadzhik SSR |

Note: "0" and "N" mean assigned depths of 0 and 33 km. respectively.

Statistics from Preliminary Determination of Epicenters, National Earthquake Information Service.

Figures 4.1 and 4.2 are plots of seismograms for various presumed explosions and earthquakes, with phases identified by time of arrival and polarization. These give an idea of the signal-to-noise ratios to be expected for various event sizes and types, and some idea of the character of the background noise on the records.

Figures 4.3 and 4.4 concentrate upon the excitation of P and PP waves for earthquakes as contrasted with explosions, and the same for vertically and horizontally polarized waves of the S-type. The principal substantive conclusion from this study up to this time is that then only useful long-period body waves to be seen from the presumed explosions are waves of the SV type, and that they probably originated as S waves at or near the source. This subject will be dealt with below.

Figure 4.5 illustrates S- waves from presumed explosions as recorded on several instruments. Even though the signal-to-noise ratios are rather low, a strong case can be made for the appearance of identical wave forms on the various records. The wave form associated with SV-type waves can be seen to have prograde elliptical particle motion in all cases, with normal dispersion. Such waves fit the definition of the shear-coupled PL waves described by Oliver and Major ( ) and as in the case of earthquakes, these waves are more prominent on the records than the true S phase itself. It is noteworthy that a phase arriving at the time of PS is prominent particularly at distances beyond 90°; as S is lost in the shadow of the earth's core, PS takes the place of S as the

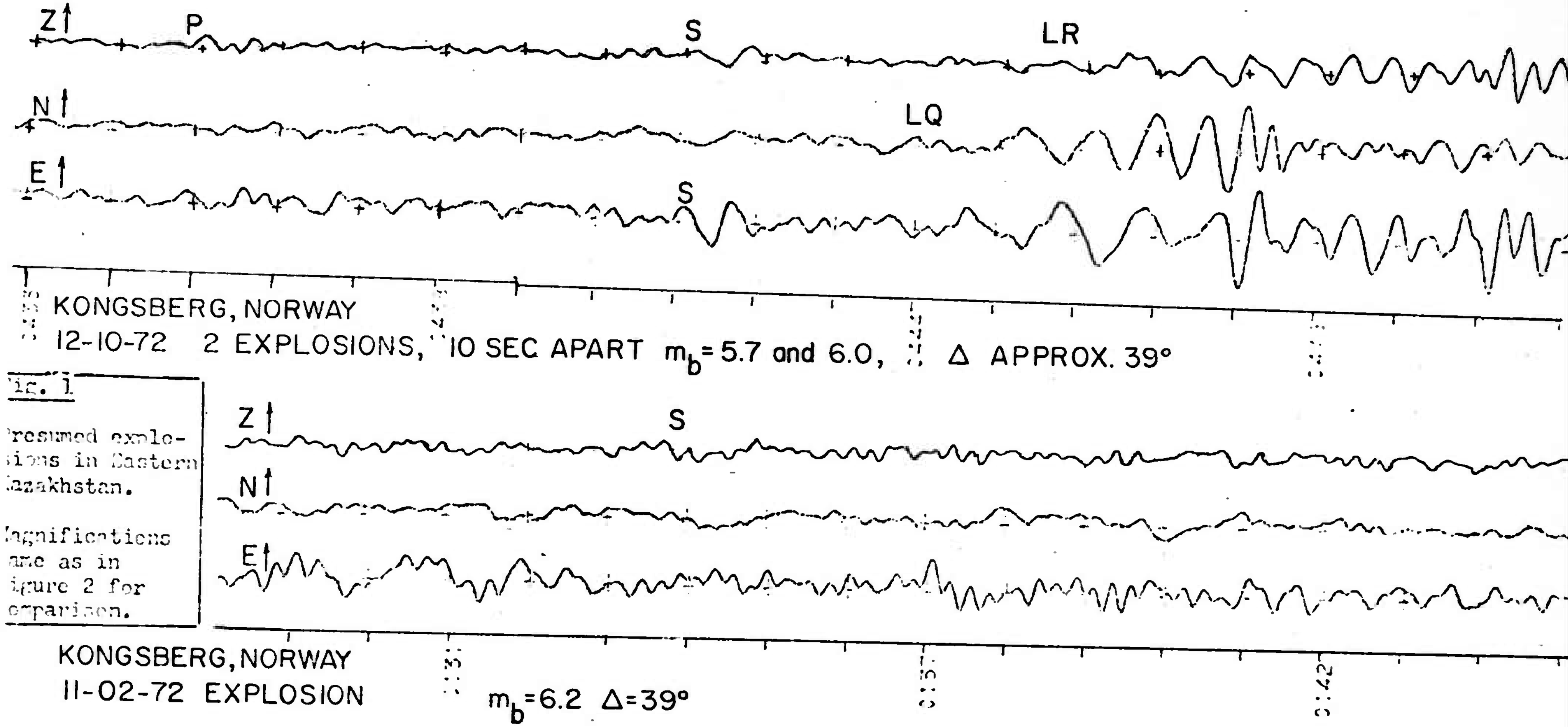


Fig. 4. 1. Raw records from the HGLP station at Kongsberg, Norway. Two presumed underground explosions from eastern Kazakhstan, USSR, are shown to demonstrate the typical amplitudes of body waves from explosions of $m_b$ around 6. Compare with the earthquakes at about the same distance in Fig. 2. The magnifications are the same in figs. 1 and 2, in order to convey the point (not unexpected, of course) that long-period body waves produced by explosions are smaller than those produced by earthquakes, typically.

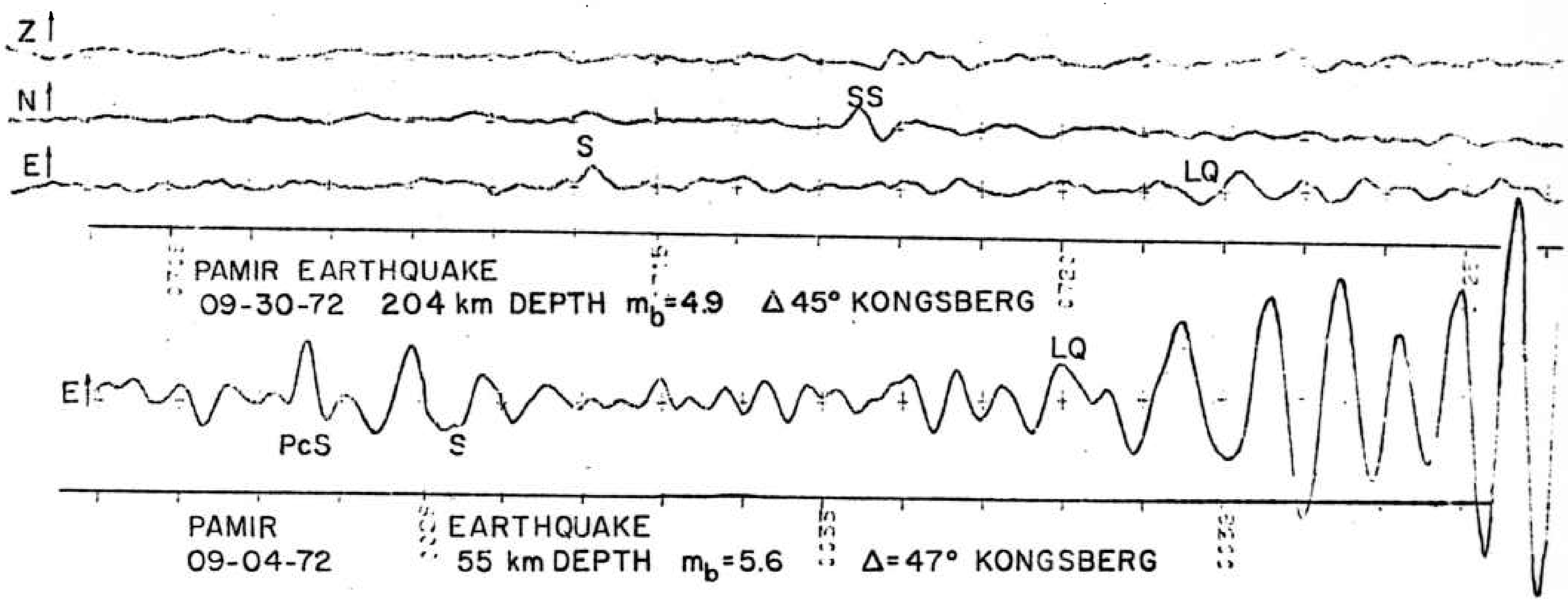


Fig. 4.2. Earthquakes in the Pamir region for comparison with the presumed explosions depicted in figure 1. Note that in the upper example good body waves are detectable at this magnification and noise level for an earthquake of $m_b$ as small as 4.9. In the lower example an earthquake of $m_b$ 5.6 has well developed long-period body-waves and relatively large surface waves compared to the substantially larger explosions (in terms of $m_b$) in figure 1. Magnifications at Kongsberg, Norway KLP station are the same in figure 1 and figure 2.

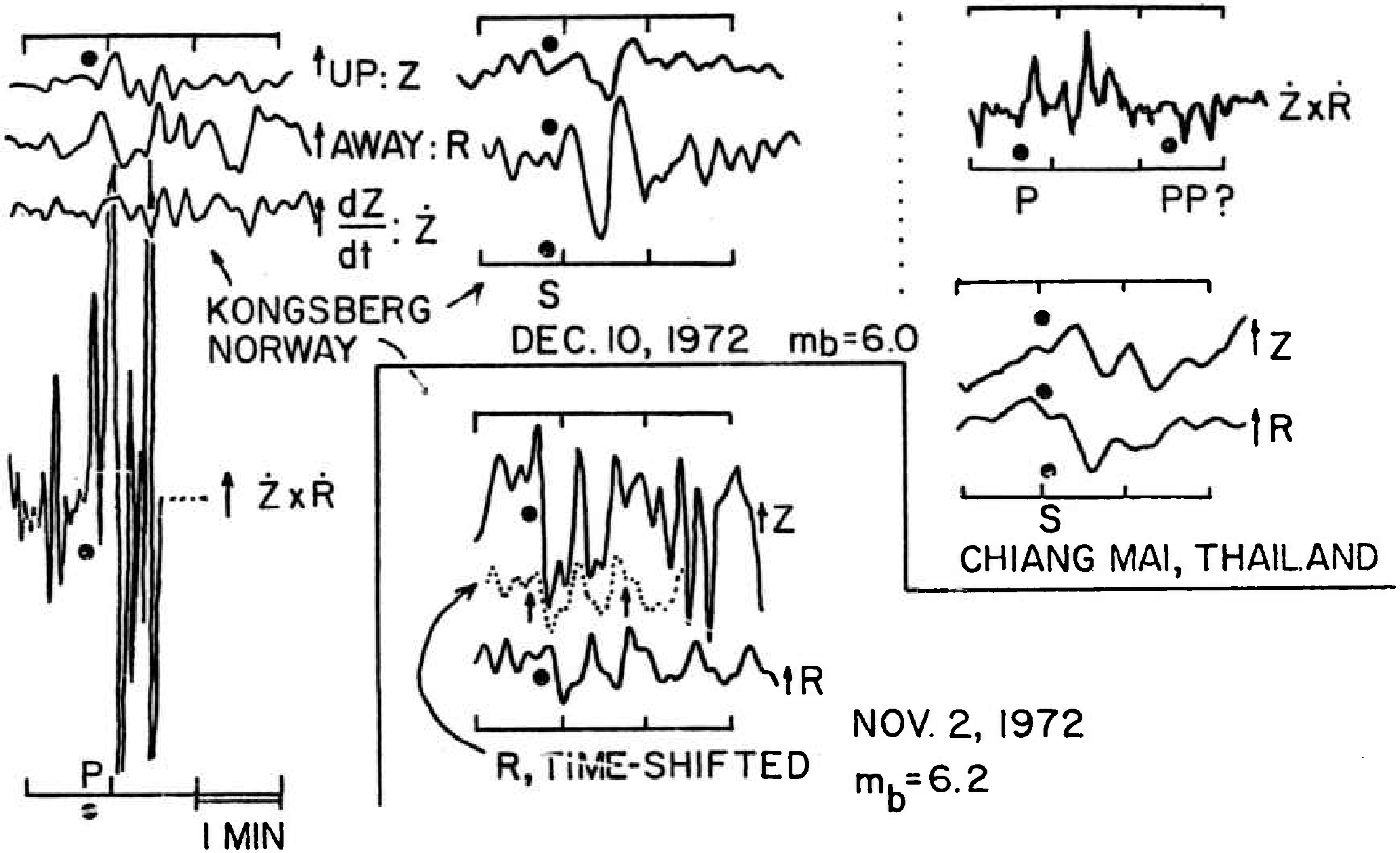


Fig. 4. 3. P and S waves from explosions and their detectibility without filtering. Horizontal components rotated into radial (R) and transverse components. The Dec. 10, 1972 event is actually two events about 10 sec apart, $m_b$ = 5.7 and 6.0. For both P and S the normally dispersed, prograde elliptical character of the particle motion (characteristic of PL waves) is evident from the pictures. Because P + pP is theoretically deficient in low frequency energy, differentiation in time is used as a crude high-pass filter. The product of the dZ/dt and dR/dt traces, given the SV polarization of the ground motion in the PL phase is then an especially sensitive indicator of this type of motion. For the Nov. 2, 1972 event the signal-to-noise ratio is much lower. Nevertheless coherence of Z and R and the characteristic ¼ period phase lead of R permit $PL_S$ to be identified. The dotted trace is R with a ¼ period phase shift to emphasise the coherence between Z and R.

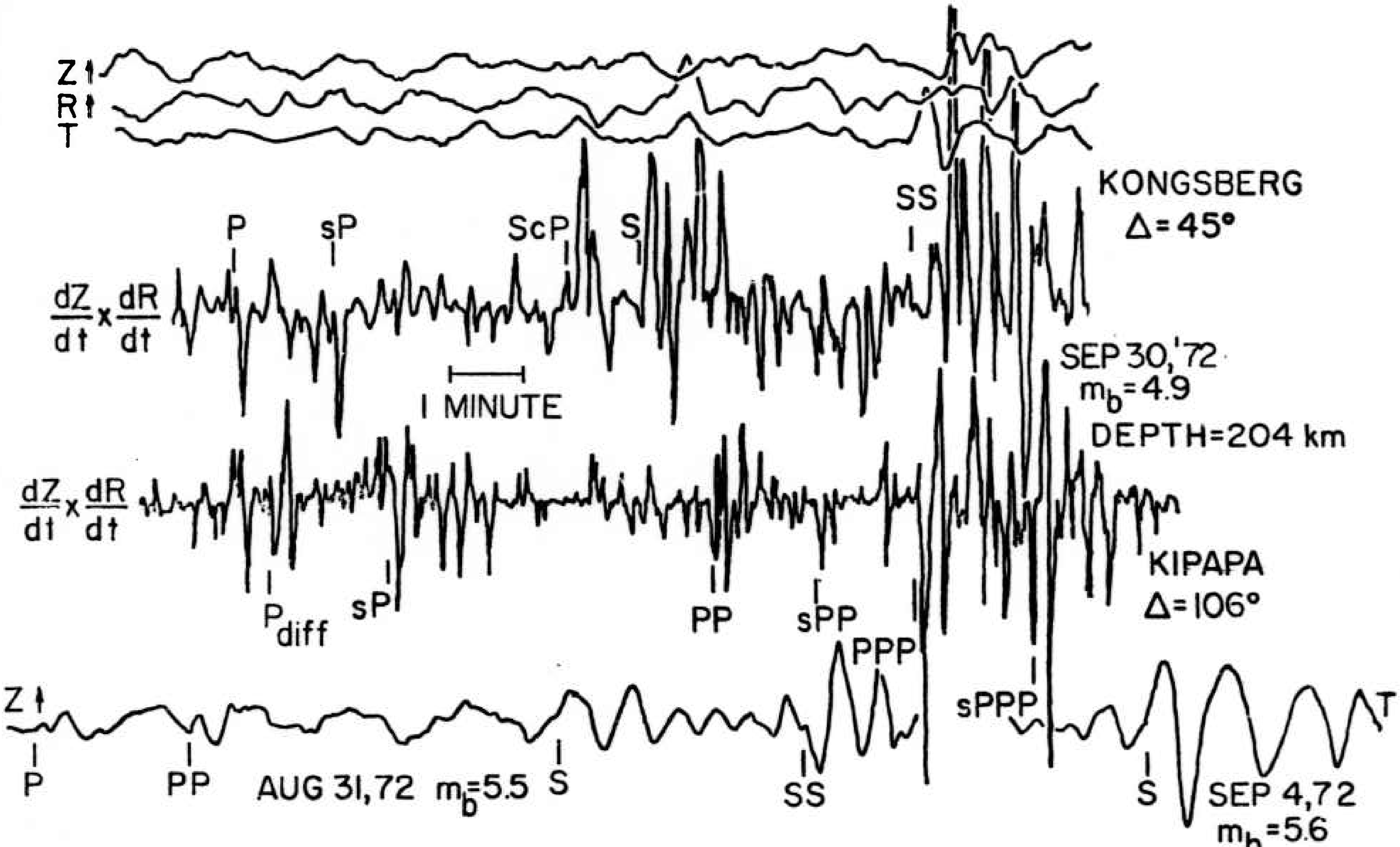


Fig. 4.4. Body waves from small earthquakes. Upper traces are the rotated but unfiltered records at Kongsberg from an earthquake of mb 4.9 at 200 km depth. Fourth trace is the product of the time-derivatives of the Z and R traces, showing the greatly increased detectability of body phases. Fifth trace is the same for Kipapa, Hawaii, at 106 degrees distance. Detection of body waves from such a small earthquake at this distance is regarded as significant. A phase shift of one of the components by ¼ period to compensate for the elliptical particle motion would produce considerably more signal amplitude in the product trace. The bottom trace shows the unfiltered vertical trace for an earthquake of $m_b$ = 5.5 ($M_s$ = 4.9) north of Mongolia, illustrating that at this magnitude body waves from earthquakes are detectable on the long period trace without complicated processing.

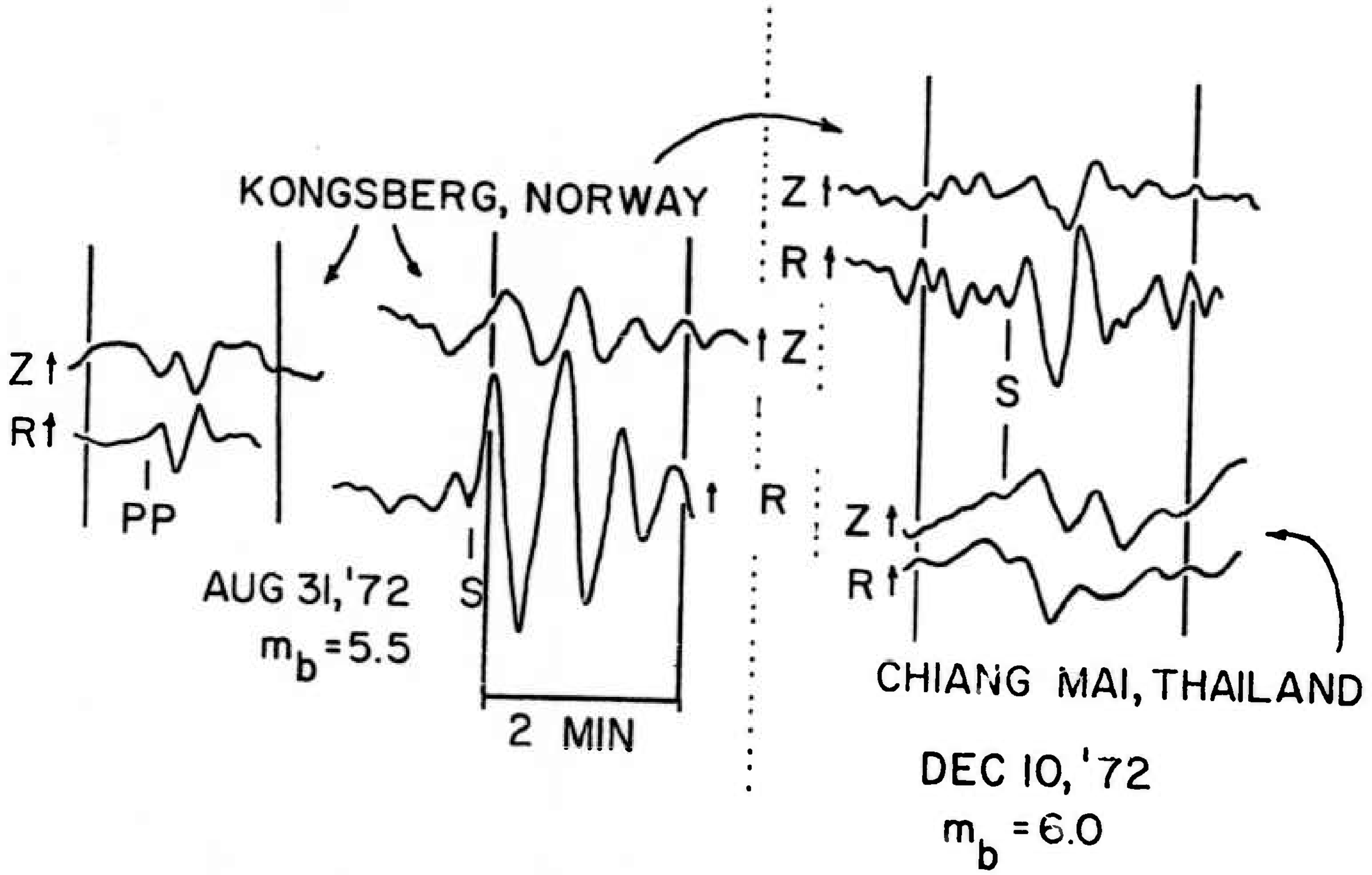


Fig. 4.5. Samples of long period body waves from an earthquake and an explosion to demonstrate the prograde elliptical particle motion observed. Magnifications are the same at Kongsberg for the two events, giving a rough idea of the relative excitation of S waves by a magnitude 5.5 ($m_b$) earthquake and a magnitude 6 ($m_b$) explosion. Motion on the transverse components (not shown) is very small, indicating SV polarization of the motion. Distance to Kongsberg is about 45 degrees for both events. Chiang Mai is about 30 degrees distant from the Dec. 10 event. The wave forms appear very similar at the two stations for the Dec. 10 event, despite quite different epicentral distances.

principal body phase, again showing the PL wave character. If, as seems likely, the phase is actually SP (initial long-period P waves being unlikely as explained previously), then the energy would appear to be transmitted primarily as P- coupled PL. Actually this question is indeterminate at present, since only circumstantial arguments about the generation of S waves are available on the basis of data in hand.

The last part of this section is dedicated to a discussion of a novel theory of shear-wave energy generation by underground explosions. It is an ad-hoc theory developed as a consequence of the observed long-period SV energy from presumed explosions. Many of the predictions of the theory are similar to those of the theory that S- waves arise from conversion of P waves at inhomogeneities in the vicinity of the explosion. A test of the theory is available, however, and this will be a task of the immediate future. The substance of the theoretical argument, a qualitative one only at this point, follows.

The argument as originally posed relates to the fact that the 'lithostatic' stress state in a rock medium under gravitational stress is not necessarily a hydrostatic stress state. An easy way to see this is to imagine a small cylinder of rock. When the cylinder is isolated, or free on all sides, it may be imagined to be in a hydrostatic stress state at zero pressure, neglecting gravity effects within the cylinder. Locked-in stresses are not considered. Next, consider this cylinder to be at the surface of a half space. If a uniform overburden is now

imposed upon the half space, the imaginary cylinder will shorten in the vertical direction, but it will be prevented from freely expanding in the lateral direction by the surrounding material. It is then clear that the cylinder is subjected to a lateral stress at depth which exceeds the overburden (vertical) stress component by the factor $\nu(1-\nu)$, where $\nu$ is Poisson's ratio for the material. If one then subtracts the hydrostatic pressure $\rho gh$, the deviatoric shear stress is of the form shown in figure 4.6a that is, a shearing stress of the order of 30-40% of the overburden stress is likely to be present at depth in the earth even in the absence of the so-called "teconic Stress" which has been invoked to explain such things as the Love wave radiation observed from explosions in Nevada[2,3]. This is not to say that that type of tectonic stress may not be present, but rather that it need not be invoked on an ad hoc basis to explain observed shear energy. When the explosion is fired it immediately forms a gas-filled cavity several meters to perhaps a hundred meters or more in diameter. Naturally the gas cannot support the pre-existing shear stress and the surrounding medium must adjust elastically in shear to attain equilibrium again. Actually the adjustment of stress amounts to a collapse in shear of the cavity, but since the 'cavity collapse' has come to denote a quite different phenomenon in the case of underground explosions, one which occurs at least minutes or hours after explosions, this deformation will be termed "cavity readjustment". An originally spherical explosion cavity will be transformed to an oblate spherioidal cavity with its short axis vertical, consonant with the lithostatic pre-stress. See

figure 4.6b. The readjustment would be expected to occur instantaneously.

The elastic readjustment of the newly created cavity has several interesting features. One feature is that the first motion of P waves from this source in roughly vertical directions will be dilatational, in contrast to those of the explosion. Secondly, the source region for the seismic radiation from the readjustment, being the zone of whole rock surrounding the cavity, has effective radius at least as large as that of the equivalent cavity due to the explosion itself. This would be expected to affect the frequency spectrum of the resulting radiation. Inelastic effects, including plastic or viscoelastic effects, and diffusion of gases through the fractured medium surrounding the explosion might drag out the completion of the process, which would undoubtedly have an adverse effect upon the radiation of higher frequencies.

Figure 4.7 indicates the 'focal mechanism' of the elastic readjustment expressed in terms of first motions. As mentioned above, the first motion of P waves in near-vertical directions will be dilatational. The polarization and the first motion of the S- waves can also be predicted. From the figure, it can be seen that the initial motion of S will be up and toward the source for teleseismic arrivals, and the surface reflection sS would arrive at a teleseismic station with the same sense. Given that the symmetry of the simple problem should be cylindrical, the S motion should be of pure SV polarization. Although in vertical cross section the mechanism is of the double couple type, it is a figure of revolution about the vertical axis, which

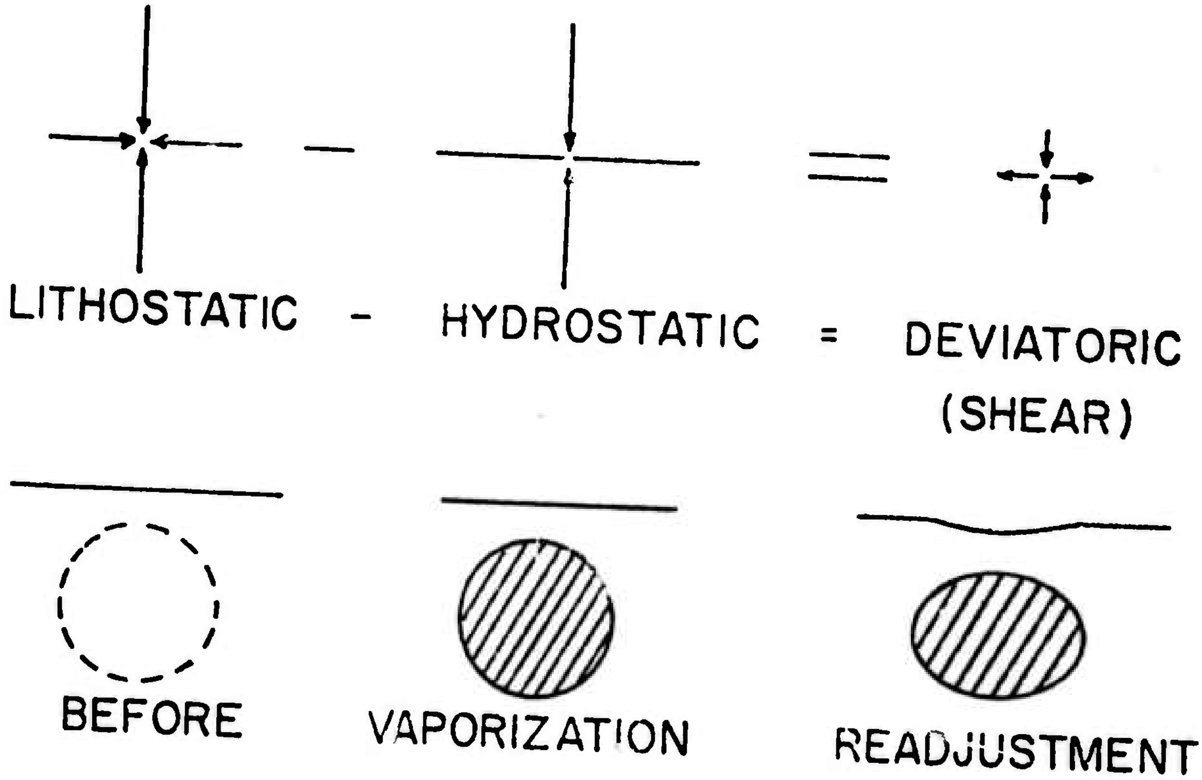


FIGURE 6a

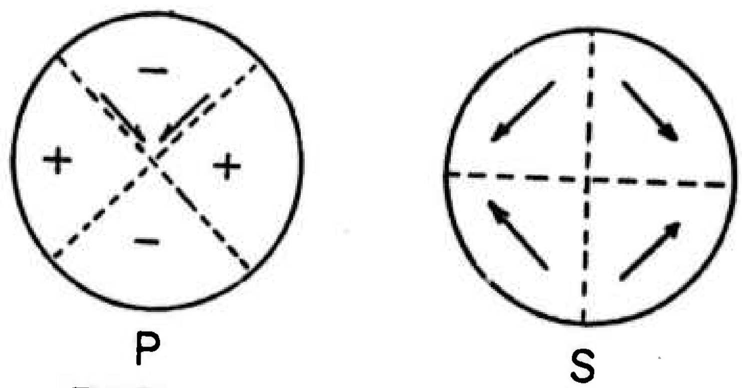


FIRST MOTION DIAGRAM
(CROSS SECTION)

FIGURE 6b

Fig. 4.6. A. Upper part shows the shear component of the 'lithostatic stress' by subtraction of the hydrostatic component. Lower part shows the collapse of the originally spherical gas-filled cavity produced instantaneously by the explosion, in response to failure of the shear modulus within the cavity. The collapse of the free surface is shown schematically; it should be expected.

B. First motion diagram for P and S phases of the <u>cavity readjustment</u> phenomenon. Cross section of a figure of revolution about the vertical.

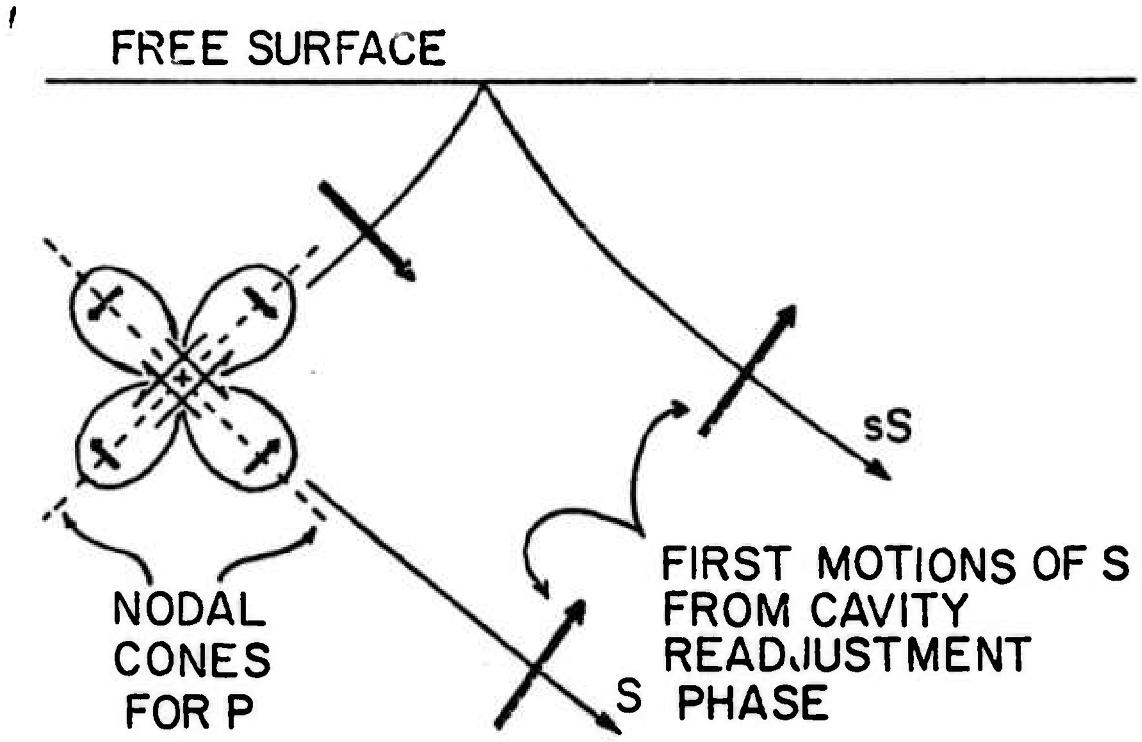


Fig. 4.7. Typical ray paths of sS and S phases produced by the cavity readjustment. The salient point is that S and sS are in phase at most teleseismic recording stations, in contrast to the case of pP and P from both the explosion and cavity readjustment, which are out of phase and hence tend to cancel one another at long periods. The spectrum of sS + S should have modulation appropriate to the sS - S time with a maximum at zero frequency. S + sS should have substantial energy at long periods as is observed. The rosette shows the amplitude distribution for S. Since the elastic cavity readjustment process has cylindrical symmetry, the drawing shows a cross-section of a figure of revolution about the vertical axis.

predicts that the first motion pattern would be a function of distance and not of azimuth. Fortunately a definitive test of the proposed model is available, since it predicts that the amplitude spectrum of the 'S' phase would have a maximum at zero frequency, and a first minimum at $1/(2\,\Delta T_s)$, where $\Delta T_s$ is the sS-S time interval appropriate to the depth of the explosion. A detailed study of this hypothesis is a primary goal of future efforts.

It appears that the project to study long period body waves of underground explosions, has produced some rather intriguing results. In particular the long period S- wave radiation from explosions, manifest primarily in particle motion of the PL type (normally dispersed, prograde elliptical, SV polarized) is surprisingly prominent. The meager observational data support a novel theoretical model which includes the elastic readjustment in shear of the medium surrounding the explosion cavity, without the necessity of the type of 'tectonic' pre-stress that has been invoked in the past. Predictions of first motion direction and pattern, including independence of azimuth, can be tested and should be valuable additions to the suite of techniques for discrimination of explosions. On the other hand, long period body waves can be more easily studied for known earthquakes of substantially smaller magnitude $m_b$, since they seem to be more strongly excited by earthquakes. A relative excitation criterion resembling the well known $M_s/m_b$ criterion appears feasible for long period body waves vs $m_b$ (for example).

The future direction of the research will be to apply record processing techniques to enhance the detectibility of the long period SV body waves of the PL type, and to study their spectra.

References.

1. Oliver, J., and M. Major, Leaking modes and the PL phase, Bull. Seis. Soc. Am. 50, 165-180, 1960.

2. Aki, K., P. Reasenberg, T. De Fazio, and Yi-Ben Tsai, Near-field and far-field evidences for triggering of an earthquake by the Benham explosion, Bull. Seis. Soc. Am. 59, 2197, 1969.

3. Boucher, G., Local seismic phenomena in the first three seconds after underground nuclear explosions, Jour. Geophys. Res. 78, 1348-1360.

## 5. Classification of Asian Earthquakes

R. Ganse and G. Lundquist

During the six months covered by this report, a seismogram digitizing system and associated computer software have been established with which to obtain magnitudes, focal mechanisms, and seismic source spectra from earthquake seismograms. Some thirty shallow Asian events were selected for study in four areas bounded by $40^\circ$ - $45^\circ$ N and $70^\circ$ - $80^\circ$E; $29^\circ$ - $35^\circ$ N and $91^\circ$ - $96^\circ$ E, $36^\circ$ - $38^\circ$N and $94.5^\circ$ - $97.5^\circ$, and $50^\circ$ - $56^\circ$N and $104^\circ$- $113^\circ$E.

### Earthquake Magnitudes.

Three separate magnitudes are computed from every available record of each event. Surface wave magnitudes, $M_s$, are computed from long-period, vertical records using the International Association of Seismology and Physics of the Earth's Interior (IASPEI) formula.

$$M_s = \log_{10}\left(\frac{\text{amplitude}}{\text{period}}\right) + 1.66 \log_{10} \Delta + 3.3,$$

where the amplitude and period are those of the largest wave in the period range 17 to 23 seconds. Long period body wave magnitudes $m_B$ are computed according to

$$m_B = \log_{10}\left(\frac{\text{amplitude}}{\text{period}}\right) + \overline{Q} \ (h, \Delta),$$

where amplitude is measured from peak to baseline on the first half cycle of the P- wave motion on the long-period vertical component seismograms.

$\overline{Q}$ (h, Δ) is Gutenberg and Richter's well-known empirical correction for distance and depth. Short period body wave magnitude $m_b$, is defined by

$$m_b = \log_{10}\left(\frac{\text{amplitude}}{\text{period}}\right) + \overline{Q}\ (h, \Delta),$$

using the maximum peak-to-peak amplitude found in the first 3 ½ cycles of P- wave motion on the short period vertical seismogram. In addition, $m_b$ and $M_B$ are to be computed for the main phase of any events judged to be a multiple event. To date, magnitudes have been computed for about one-fourth of the events selected, and the results are not inconsistent with worldwide $m_b$ - $M_s$ relationships. However, results are much more consistent than other published magnitudes for the same events, probably due to personal reading of seismograms, and application of a broader data base for each event.

Preliminary b values have been prepared for the areas under study using magnitudes published by NEIC. However, the number of events is too small to make such determinations statistically significant in three of the four areas.

Body Wave Focal Mechanisms.

Focal mechanisms are determined from P- wave first motions, and S- wave polarization angles. Some P- wave first motions have been gathered from the ISC Bulletin, but primary emphasis is placed upon readings gathered specifically for this study. S- wave horizontal particle motion diagrams are constructed for all S waves digitized for spectral

analysis. Experience so far indicates that one or two good S- wave polarization angles can be critically important in distinguishing between possible P- wave focal mechanism solutions. A catalogue of predicted P- and S- wave motions for all possible double-couple sources (provided by Mr. Wm. Dillinger of the USGS) will be used to aid in this part of the study.

Tentative focal mechanisms based on a combined P and S solution for one event and P solutions for three other events in the area bounded by 29° - 35° N and 91° - 96° E are of consistent strike-slip character. The solution will be refined using further S- wave data and Russian seismograms as available. One combined P and S wave focal mechanism in the area bounded by 40° - 45° N and 70° - 80°E agrees with the predominantly thrust focal mechanisms with roughly north-south compression published by Molnar, et. al., for that area. Consistent published solutions could not be found for the other area.

Seismic Source Spectra.

Body-wave source spectra are computed from both short and long period WWSSN seismograms. Seismograms from the USSR network have been ordered and spectra will also be derived from these. Raw P- wave spectra are obtained by digitizing and Fourier-transforming vertical component records. The S- wave spectra are computed from the transverse component of the S- wave, as obtained from the N-S and E-W components by an axis rotation.

The raw spectra are corrected for instrument response (to get station ground-motion spectra) and then for anelastic attenuation. The resulting quasi-source spectra will be averaged over eight or more stations with good azimuthal distribution to give the final earthquake spectrum. Seismic moment, stress drop and fault length will be estimated from spectra of sufficient quality.

Although P- wave source spectra are fairly insensitive to the choice of Q, the locations of the S- wave corner frequencies are highly dependent upon the anelastic attenuation model used. Separate meaned quasi-source spectra were constructed by applying the attenuation versus frequency corrections predicted by the velocity model CIT 11 CS2 and Q model QM (low Q)[2] and CIT 208 (high Q)[3] model. On the basis of compatibility of the P- and S- wave spectra, results from four events seem to favor the CIT 208 model. An example of the spectra for the different models is shown in Fig. 5. 1.

References.

1. Molnar, P., T. J. Fitch, and F. T. Wu, Fault Plane Solutions of Shallow Earthquakes and Contemporary Tectonics in Asia, Earth and Planetary Science Letters, 19: 101-112, 1973.

2. Anderson, D. L., Latest information from seismic observations, chapter 12 in The Earth's Mantle, (T. F. Gaskell, editor), pp 355-420, Academic Press, 1967.

3. Julian, B. personal communication.

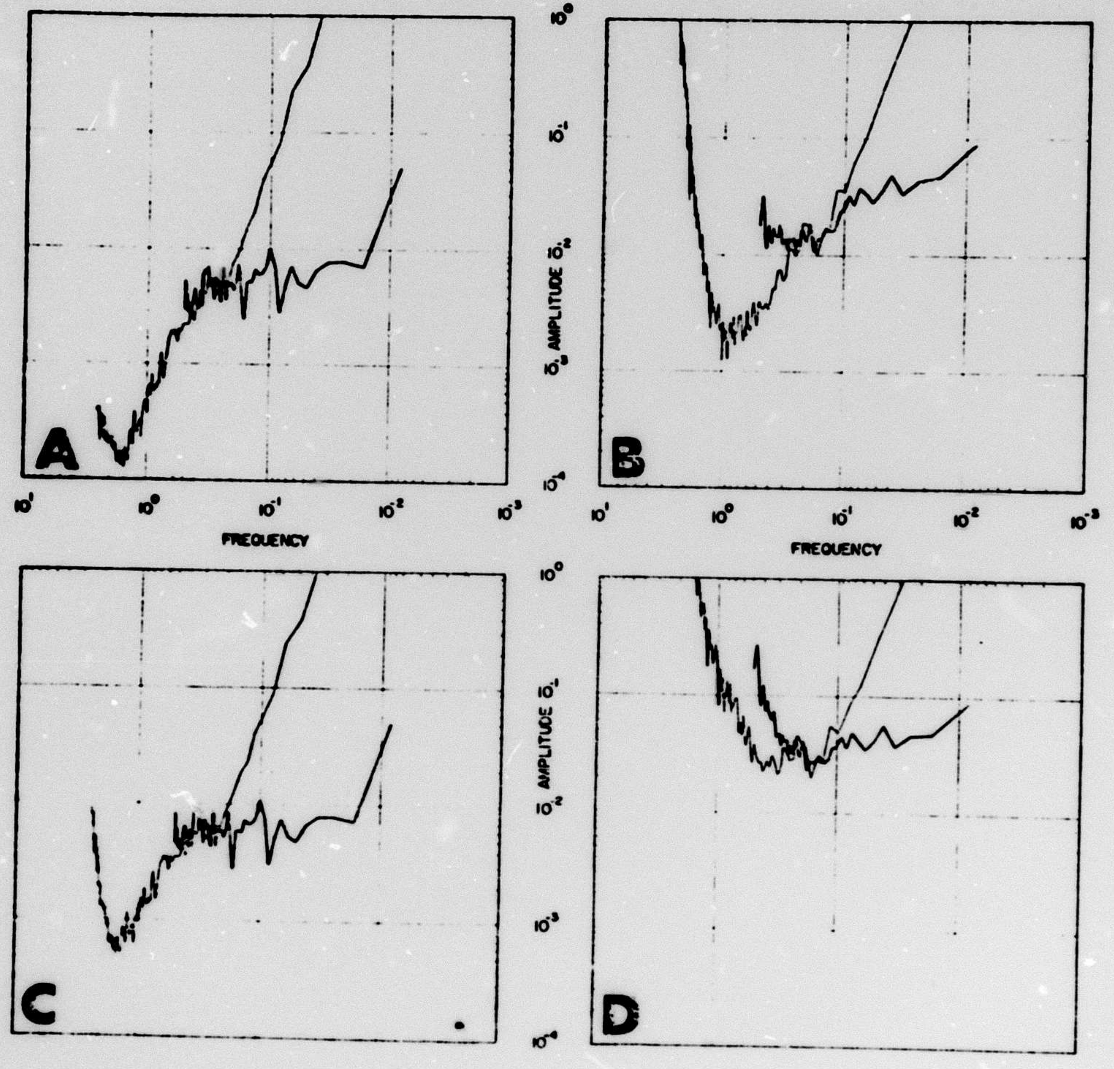


Fig. 5.1 Mean "Quasi-source spectra" (station spectra corrected for anelastic attenuation) for 3 April 1971 event. Heavy line is spectrum determined from long period seismograms; light line is spectrum determined from short period seismograms. Diagram A is P- wave spectrum corrected by CIT 208 attenuation model; B is S- wave spectrum corrected by CIT 208; C is P- wave spectrum corrected by CIT 11 CS2-QM; D is S- wave spectrum corrected by CIT 11 CS2-QM.